Journal Pre-proofs

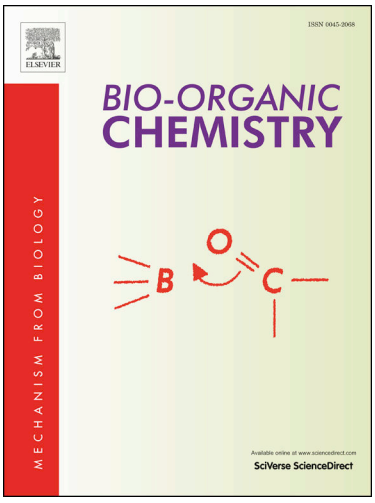

Design and synthesis of pinane oxime derivatives as novel anti-influenza agents

Jianghong Dong, Mengjie Xiao, Qinge Ma, Guicheng Zhang, Weijie Zhao, Mengjie Kong, Yue Zhang, Luyun Qiu, Wenhui Hu

PII: S0045-2068(20)31403-6
DOI: https://doi.org/10.1016/j.bioorg.2020.104106
Reference: YBIOO 104106

To appear in: *Bioorganic Chemistry*

Received Date: 3 May 2020
Revised Date: 26 June 2020
Accepted Date: 14 July 2020

Please cite this article as: J. Dong, M. Xiao, Q. Ma, G. Zhang, W. Zhao, M. Kong, Y. Zhang, L. Qiu, W. Hu, Design and synthesis of pinane oxime derivatives as novel anti-influenza agents, *Bioorganic Chemistry* (2020), doi: https://doi.org/10.1016/j.bioorg.2020.104106

Design and synthesis of pinane oxime derivatives as novel anti-influenza agents

Jianghong Dong [a, *], Mengjie Xiao [c], Qinge Ma [d], Guicheng Zhang [e], Weijie Zhao [a], Mengjie Kong [a], Yue Zhang [a], Luyun Qiu [a], Wenhui Hu [b, *]

[a] College of Chemistry and Pharmaceutical Engineering, Huanghuai University, Zhumadian 463000, China

[b] State Key Laboratory of Respiratory Disease, Key Laboratory of Molecular Target & Clinical Pharmacology, School of Pharmaceutical Sciences, Guangzhou Medical University, Guangzhou 511436, China

[c] School of Life Sciences, Chinese University of Hong Kong, Shatin, N.T, Hong Kong, SAR 999077, China

[d] Key Laboratory of Modern Preparation of TCM of Ministry of Education & Research Center of Natural Resources of Chinese Medicinal Materials and Ethnic Medicine, Jiangxi University of Traditional Chinese Medicine, Nanchang 330004, China

[e] Guangzhou Institutes of Biomedicine and Health, Chinese Academy of Science, 190 Kaiyuan Avenue, Guangzhou 510530, China

Address correspondence to these authors:

Jianghong Dong, Ph.D.

College of Chemistry and Pharmaceutical Engineering, Huanghuai University, Zhumadian 463000, China

E-mail: hndxdjh555@163.com

Wenhui Hu, Ph.D.

State Key Laboratory of Respiratory Disease, Key Laboratory of Molecular Target & Clinical Pharmacology, Guangzhou Medical University, Guangzhou 511436, China

E-mail:huwenhui@gzhmu.edu.cn

Abstract

Parasitic characteristics, mutations and resistance of influenza A virus make it difficult for current influenza antiviral drugs to maintain long-term effectiveness. Currently, to design non-adamantane compounds targeting the S31N mutant of M2 proton channel is a promising direction for the development of novel anti-influenza drugs. In our previous research, a pinanamine-based antiviral **M090** was discovered to target hemagglutinin instead of M2, with its structure being highly similar to reported M2-S31N inhibitors. Herein, a series of pinane oxime derivatives were designed from scratch and evaluated for anti-influenza activity and their cytotoxicity *in vitro*. Utilizing a combination of structure-activity relationship analysis, electrophysiological assay and molecular docking, the most potent compound **11h**, as a M2-S31N blocker, exhibited excellent activity with EC_{50} value at the low micromolar level against both H3N2 and H1N1. No significant toxicity of **11h** was observed. In addition, compound **11h** was located tightly in the pore of the drug-binding site with the thiophene moiety facing down toward the C-terminus, and did not adopt a similar position and orientation as the reference inhibitor.

Keywords: Influenza A virus, Amantadine-resistant, S31N mutant, Pinane oxime derivative, antiviral drug

ABBREVIATIONS

M2, matrix-2 protein; S31N, Serine 31 arganine; WT, wild type; EC_{50}, half maximal effective concentration; TC_{50}, 50% cytotoxic concentration; NOE, Nuclear Overhauser effect; CPE, cytopathic effect; NMR, nuclear magnetic resonance; MTT, (3-(4,5-Dimethylthiazol-2-yl)-2,5-Diphenyltetrazolium Bromide; SAR, structure-activity relationship; DMF, N,N-dimethylformamide; RMSD, root mean square deviation; TosMIC, tosylmethyl isocyanide; PDC, pyridinium dichromate; TBTU, 2-(1H-benzotriazole-1-yl)-1,1,3,3-tetramethyluronium tetrafluoroborate; DMSO, dimethyl sulfoxide; $SOCl_2$, thionyl chloride; TLC, thin layer chromatography; $CDCl_3$, chloroform-*d*; AMD, amantadine; IFD, induced fit docking; PDB, Protein Data Bank; MDCK, Madin-Darby canine kidney; PBS, phosphate buffered saline; DMEM, Dulbecco's modified Eagle medium.

1. Introduction

Influenza viruses are highly pathogenic microorganisms that cause acute respiratory diseases and are responsible for the recurrent seasonal epidemics and occasional pandemics, which seriously endanger human health [1, 2]. Currently, the best way for prophylaxis of influenza is to get vaccinated each year. However, due to the production and manufacturing limitations of pharmaceutical companies, the initial supply of the vaccines might not be enough to meet the demand for them [3]. Various types and strains of pathogenic viruses are constantly adapting and developing resistance to medications and treatments. Therefore, influenza vaccines should be updated annually based on rigorous international surveillance and scientists' estimations [4]. These prevention factors are highly effective at minimizing influenza pandemics. It is also worth noting that once patients are infected with influenza viruses, they will be promptly treated with antiviral medications to shorten the duration of illness symptoms and reduce complications [5].

Influenza antiviral drugs, approved by the U.S. Food and Drug Administration (FDA), include three classes: virion ion-channel (M2 protein) inhibitors (amantadine and rimantadine), neuraminidase inhibitors (oseltamivir, zanamivir and peramivir) and cap-dependent endonuclease inhibitor (baloxavir marboxil) [6]. Indeed, the parasitic nature of influenza virus and its susceptibility to spontaneous mutations make it difficult for chemical drugs to have a long-lasting effect. For example, drug resistance of amantadine, oseltamivir and other first-line drugs emerged in varying degrees [7]. Antiviral resistance to baloxavir is currently very low, but this has already happened [8]. In this regard, there is an urgent need for development of new anti-influenza drugs.

Classical M2 inhibitors (amantadine and rimantadine, Fig. 1 and Fig. 2)) are rarely used because the M2-S31N mutant in more than 95% of clinically isolated influenza A viruses makes those drugs difficult to bind [9]. Thus, it appears that it is logical and valid to design non-adamantane-based M2-S31N inhibitors to address the problem of adamantane resistance. For one thing, the crystal structure of the S31N mutant has recently been reported, and it is possible to study the structural function and drug-

resistant mechanisms of the mutant channels with the development of molecular modeling techniques, solid (or liquid) nuclear magnetic technology and lipidic cubic phase crystallization techniques [10-12]. For another, researchers around the world have spared no effort to develop new small molecular inhibitors of M2-S31N mutant [13]. Instead, they have summarized a phamacophore structure of adamantyl-1-$NH_2^+CH_2$−aryl and a series of amantadine derivatives have been reported [14-21]. Among them, compound WJ332 (Fig. 1) is the first M2-S31N inhibitor as amantadine derivative and compound **1** (Fig. 1) exhibits favorable absorption, distribution, metabolism, excretion, and toxicity (ADMET) properties and antiviral activity *in vitro* [20]. In addition, M2-S31N inhibitors show a higher *in vitro* genetic barrier to drug resistance than amantadine in cell culture, and drug resistance only emerges under high drug selection pressure after several passages [18, 22]. These research jobs have laid down a theoretical and realistic foundation for the development of new M2 inhibitors.

(1R,2R,3R,5S)-3-pinanamine(Fig. **2**) is a monoterpene amine that blocked the replication of wild-type influenza A virus as an M2 ion channel inhibitor identified by our research group [23]. And a series of pinanamine-based antivirals were designed and synthesized by attaching a bulky and hydrophobic functionality to pinanamine through a systematic structure−activity relationship (SAR) study [24-27]. Interestingly, an imidazole-based pinanamine derivative **2** (Fig. **1**) exhibited dual inhibitory activity against the wild-type and drug-resistant mutant of the influenza A virus [25]. The methyl group was changed to a medium-size n-propyl group to afford the compound **3** (Fig. **1**), of which M2-WT ion channel inhibition activity remained but M2-S31N ion-channel inhibition activity disappeared [26]. However, 3-cyclopropylthiophene-based pinanamine **4** (Fig. **1**, M090) was discovered to inhibit viral replication by targeting the viral hemagglutinin instead of M2-S31N mutant [27]. In addition, the same phenomenon occurred in aminoadamantanes and azapropellanes with excellent anti-influenza A virus activity through M2-S31N independent mechanisms [28, 29]. It means that subtle change in the scaffold structure of antiviral chemotherapeutic agent could lead to variety in target protein and mechanism of action.

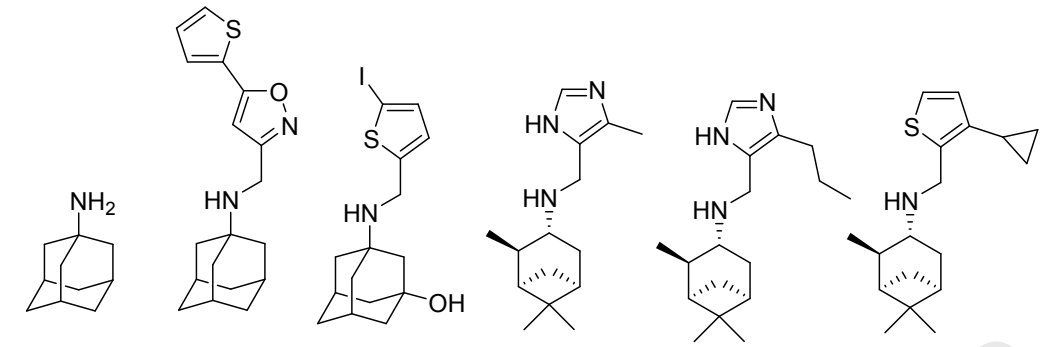

Amantadine WJ332 **1** **2** **3** **4**(M090)

Fig. 1. Structure of Amantadine, adamantane-based M2-S31N inhibitors and several reported pinanamine-based antivirals.

To address the problem of adamantane resistance and the discrepancy of pinanamine-based antivirals, the structural characteristics of rimantadine were re-examined from scratch, and a series of novel pinane oxime derivatives (Fig. **2**) were designed in the hope of specifically targeting the M2-S31N ion channel. The new synthesized compounds were assessed for their *in vitro* antiviral activity against the pandemic influenza virus A/HK/68 (H3N2, wild type, WT) and A/WSN/33 (H1N1, S31N mutant). Meanwhile, cytotoxicity of the compounds was evaluated in uninfected MDCK cells. And structure-activity relationship (SAR) was also discussed. Moreover, these efforts resulted in a promising lead compound **11h** endowed with the most potency against amantadine-sensitive, as well as amantadine-resistant influenza A viruses (EC_{50} = 3.29 μM and 2.45 μM, respectively), with a TC_{50} value over 173.14 μM. Accordingly, the compound was subjected to patch clamp assay and molecular docking to shed light on whether the observed antiviral activity was by blocking M2 ion channel and reasonable theoretical binding patterns. This study could enrich the diverse library of pinane-based compounds and provide a molecular probe for further chemical biology research.

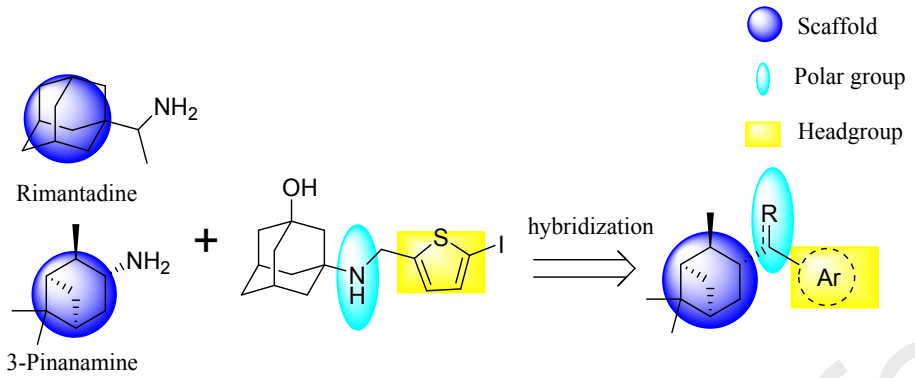

Fig. 2. Design strategy of the target compounds

2. Results and discussion

2.1. Chemistry

Synthetic routes are shown in **Schemes 1**. Using the (-)-isopinocampheol as raw material, (1*R*,2*R*,3*R*,5*S*)-2,6,6-trimethylbicyclo[3.1.1]heptane-3-carboxylic acid **6** was synthesized by oxidation of compound **5**, cyanide reaction and nitrile hydrolysis, with a 36.4% yield over three steps [30]. The carboxylic acid **6** was condensed with *N,O*-dimethylhydroxylamine hydrochloride to give Weinreb amide **7** , which was treated with the lithium reagent of various substituted thiophene or other aromatic compounds to afford the corresponding Weinreb ketones **8a-j** [31]; In another way, carboxylic acid **6** was treated with thionyl chloride in the presence of DMF to afford the acyl chloride **10**, and the compound **10** underwent smooth Friedel-Crafts acylation with different substituted thiophenes catalyzed by $SnCl_4$ to obtain the corresponding ketones **10a-d** [32]. The ketones **8a-j** and **10a-d** were transformed into the corresponding pinane oxime derivatives **11b-o** by heating with hydroxylamine hydrochloride in the presence of pyridine [33]. Among them, the geometry of pinane oxime derivative **11h** was selectively determined as anti-confirmation using ^{1}H NMR NOE spectrum. It could be seen that the 2D NOESY spectrum of compound **11h** showed strong NOE correlations between protons from the hydroxyl of oxime and the 2-methyl of pinane backbone, other than 3'-H of the thiophene moiety (Figure S1 in Supporting Information).

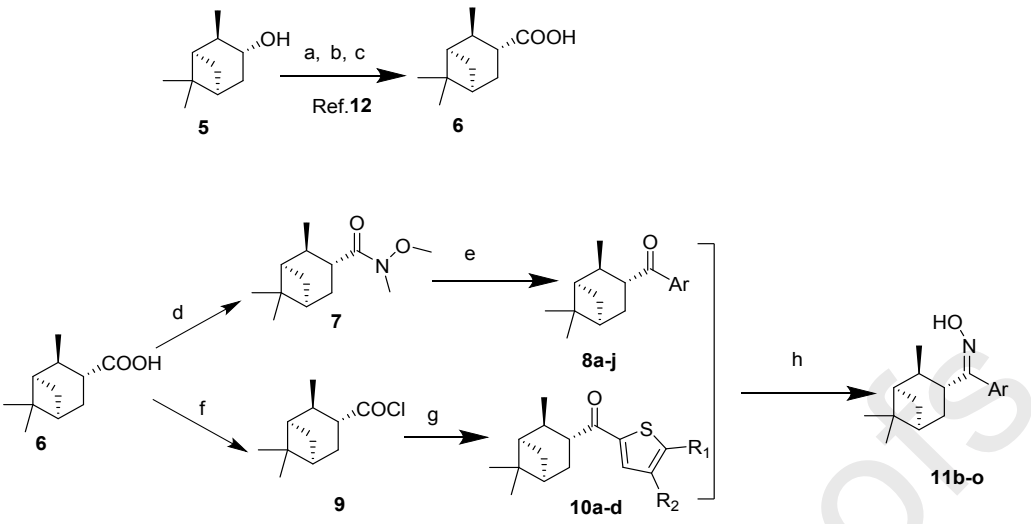

Scheme 1. Reaction Condition: (a) PDC, CH_2Cl_2, r.t., overnight; (b) TosMIC, *t*-BuOK, DMSO, 60 ℃, 48 h; (c) H_2SO_4, CH_3COOH, reflux, overnight; (d) *N,O*-dimethylhydroxylamine hydrochloride, TBTU, triethylamine, CH_3CN, r.t., 1 h; (e) Me/ArLi, ether, 0 ℃, 30 min; -78 ℃, 3 h; (f) $SOCl_2$, cat. DMF, reflux, 2 h; (g) substituted thiophene, $SnCl_4$, dry CH_2Cl_2, 0 ℃, 30 min; (h) pyridine, $NH_2OH{\cdot}HCl$, 80 ℃, 24 h.

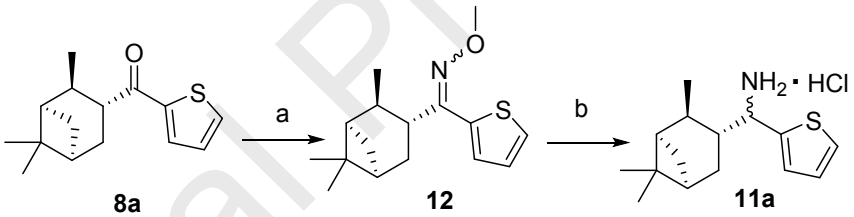

Scheme 2. Reaction Condition: (a) pyridine, methoxyammonium chloride, 80 ℃, 24 h; (b) $LiAlH_4$, diethyl ether, 0-40 ℃, 4h; HCl/ethyl acetate, r.t..

Treatment of ketone **8a** with methoxyamine hydrochloride gave O-methyl oxime **12**, which was readily reduced by Lithium aluminum hydride to a mixture of two isomeric amines **11a** (**Schemes 2**) [34]. Compound **11d** was reacted with (*S*)-*N*-Boc-2-(bromomethyl)pyrrolidine under basic conditions using sodium hydride in DMF to yield the compounds **13a** and **13b**, which were treated with hydrogen chloride/ethyl acetate solution to give the target compounds **14a** and **14b**, respectively, as hydrochlorides (**Schemes 3**) [35].

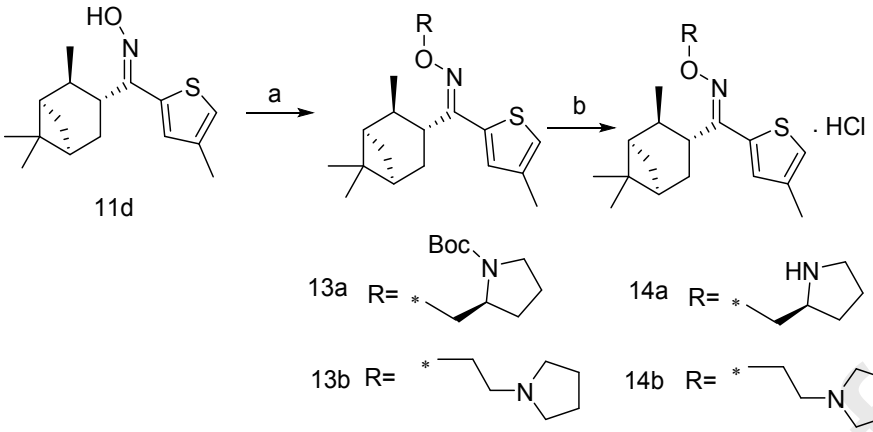

Scheme 3. Reaction Condition: (a) 60 % NaH, RBr, DMF, 0 ℃; (b) HCl/ethyl acetate, r.t.。

2.2. Viral inhibition assay

All the novel compounds were subjected to antiviral evaluation against influenza A virus including amantadine-sensitive A/Hong Kong/8/68 strain (H3N2, M2-WT) and amantadine-resistant A/WS/33 strain (H1N1, M2-S31N) in virus-infected Madin-Darby canine kidney (MDCK) epithelial cell according to a previous report [26]. In addition, cytotoxicity of the compounds was performed in uninfected MDCK cells by 3-(4,5-dimethylthiazol-2-yl)-2,5-diphenyltetrazolium bromide (MTT) assay. Amantadine (AMD) was used as the reference drug for comparison. The antiviral data (half maximal effective concentration, EC_{50}) obtained by microscopic scoring of the virus-induced CPE and cytotoxic results (50% cytotoxic concentration, TC_{50}) are presented in **Table 1**.

2.3. Structure-activity relationship

Table 1
Structures and *in vitro* inhibition efficiency of test compounds against influenza A viruses

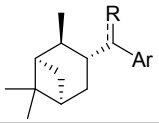			Antiviral EC_{50} [a](μM)		Cytotoxicity (TC_{50} [b], μM)
Compd.	R	Ar	A/HK/68	A/WSN/33	
11a	NH_2		0.27±0.07	NA [c]	193.23

11b	=NHOH		12.4 ± 1.2	11.8 ± 0.8	>200.46
11c	=NHOH	Me	NA	NA	>276.4
11d	=NHOH		10.8 ± 1.3	14.81 ± 2.5	93.43
11e	=NHOH	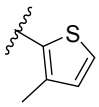	22.2 ± 3.0	NA	63.09
11f	=NHOH	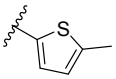	29.1 ± 3.2	11.9 ± 1.12	>191.04
11g	=NHOH	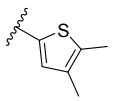	4.84 ± 0.6	30.2 ± 3.6	>154.21
11h	=NHOH	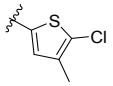	3.29 ± 0.10	2.45 ± 0.06	>173.14
11i	=NHOH	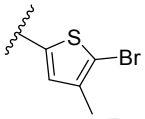	25.4 ± 1.5	19.29 ± 0.47	>154.35
11j	=NHOH	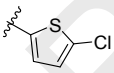	7.11 ± 0.72	5.97 ± 0.81	>191.37
11k	=NHOH	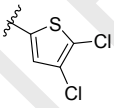	9.44 ± 0.91	10.15 ± 1.26	>162.51
11l	=NHOH	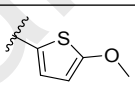	NA	18.65 ± 3.1	>170.4
11m	=NHOH		8.65 ± 0.42	32 ± 2.61	>200.46
11n	=NHOH	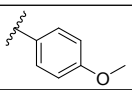	–[d]	NA	>187.89
11o	=NHOH	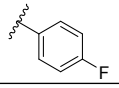	–	NA	>196.1
14a	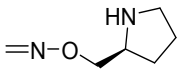	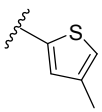	–	NA	10.15
14b	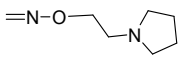	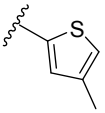	–	NA	9.67
AMD			3.7±0.6	199.9±21	337.19

Data are presented as the mean ± S.D. of the results of two or three independent tests. [a] EC_{50} represents half maximal effective concentration. [b] TC_{50} represents 50% cytotoxic concentration, as determined by the MTT cell viability test. [c] NA, no activity. [d] The symbol "–" indicates "not tested."

It has been previously found that 1-((1*R*,2*R*,5*S*)-2,6,6-trimethylbicyclo[3.1.1]heptan -3-yl)ethan-1-amine, which was similar to rimantadine, exhibited anti-influenza activity against the M2-WT virus A/HK/68 (EC_{50} = 1.93 μM) [30]. As a privileged pharmacophore, the thiophene group played a significant role in the activity against amantadine-resistant influenza virus[16, 20, 27]. Replacement of the methyl group of this compound with the thiophen-2-yl moiety afforded compound **11a**, and clearly increased the antiviral activity against WT virus, but this analogue exhibited no activity against amantadine-resistant strain A/WSN/33. Surprisingly, the corresponding oxime derivative **11b** displayed dual inhibitory activity against the M2-MT virus A/HK/68 and the amantadine-resistant strain A/WSN/33, with its EC_{50} values of 12.4 μM and 11.8 μM respectively. On the other hand, viral inhibitory potency of the methyl-substituted analog **11c** disappeared. In order to clarify the effectiveness of various substituted pinane-based thiophene oxime derivatives on the anti-influenza activity, compounds **11d–l** were synthesized by introducing simple methyl, methoxy or halogen groups. Compounds **11d** containing Ar = 4-methyl-thiophen-2-yl and **11f** containing Ar = 5-methyl-thiophen-2-yl maintained antiviral effect against the amantadine-resistant H1N1 virus while 3-methyl derivative **11e** showed no inhibition potency. The information suggested that modifying 4,5-position of thiophene was beneficial to antiviral activity. However, compound **11g** with 4,5-dimethyl group displayed inferior activity against H1N1 and superior activity against H3N2 compared with compound **11b**. Fortunately, among 2,5-disubstituted thiophene derivatives **11g-i** and **11k**, the most potent analogue **11h** exhibited almost 4-fold increased inhibitory activity against both wild-type and drug-resistant mutant of the influenza A virus compared with **11b** (EC_{50} = 3.29 μM and 2.45 μM, respectively). As reported halogenation was a valuable approach for improving ligand bioactivity [36]. Comparison of activity of compounds **11h-k** indicated that it was preferable for 5-position of the thiophene group to be substituted by electron-withdrawing chlorine atom. Introducing an electron-donating methoxy group to 5-position of the thiophene ring resulted in compound **11l**, which clearly abolished its anti-influenza activity. Replacing the thiophene moiety of **11b** with the thiazol-2-yl (**11m**), 4-methoxyphenyl (**11n**) or 4-fluorophenyl (**11o**) groups also led

to significant decline in activity or inactivity against amantadine-resistant influenza virus.

To extend the SAR information, the oxime ether derivatives **14a** and **14b** were also designed by adding a hydrophilic secondary amine or tertiary amine to compound **11d**. Unfortunately, the two designed compounds totally lost their effectiveness probably as a result of their higher cytotoxicity.

SAR analysis of the newly synthesized compounds demonstrated that the potent inhibitors could be obtained if the amine group of 3-pinanamine was substituted by the oxime group, just as other polar groups such as the hydroxyl, guanidine, amidine, or aminooxyl groups [37]. In addition, the thiophene ring was the optimal heterocycle attached to pinane to achieve the best antiviral inhibitory potency and 5-position of the thiophene moiety favored electron-withdrawing substitutions, such as chlorination. Significantly, compound **11h** bearing the 4-methyl-5-cholo-thiophene substituent proved to be promising lead compound with low cytotoxicity, inhibiting both drug-sensitive and -resistant influenza A viruses. The SAR of the synthesized compounds was summarized in Fig. **3**.

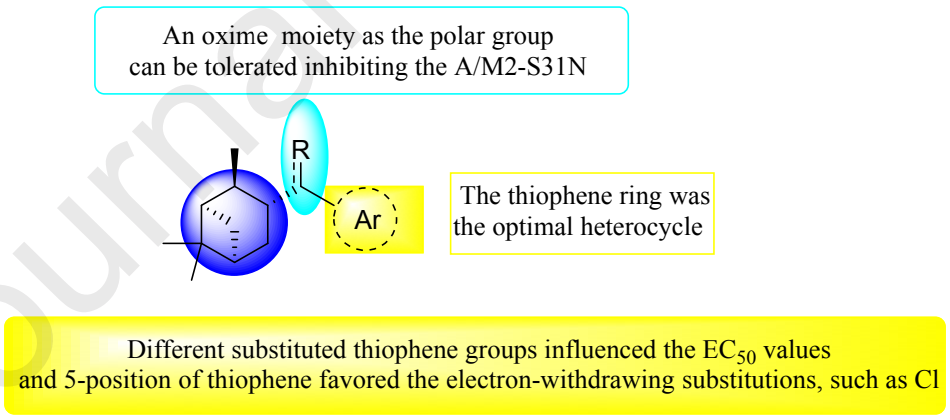

Fig. 3. A preliminary summary of SAR

2.4. Whole cell patch clamp assay

To verify whether the antiviral efficacy of the novel pinane oxime derivatives was through M2 ion channel blockage or not, patch clamp electrophysiology in mammalian cells was conducted. Compounds **11a**, **11b** and **11h** were selected and tested in the

whole cell patch clamp assay using 293T-Rex cells expressing either the M2-WT or the M2-S31N mutant of the M2 protein, as previously reported [23, 38].The percentage inhibition of currents through the M2-WT and M2-S31N ion channels at pH 5.5 was recorded in Fig. **4** after 2 min of co-applied with 100 μM of compounds. All measurements were repeated three times. The results were consistent with those of the cell-based phenotypic method.

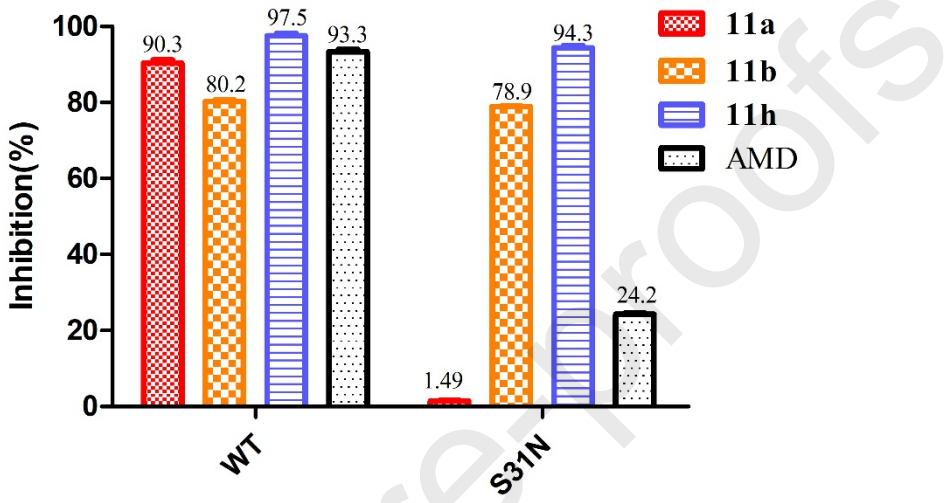

Fig. 4. Inhibition of the M2 WT and S31N ion channel conductivity by various compounds as determined by patch clamp assays.

2.5. Molecular docking study

To figure out the binding modes of the pinane oxime derivatives with the active site of the M2-S31N channel, Schrödinger's induced fit docking (IFD) protocol [39] was performed by using the solution NMR structure of M2-S31N (PDB ID code: 2LY0 [15]) as the template. Based on the *in vitro* inhibition results, compounds **11a**, **11b** and **11h** were selected as ligand examples. Utilizing molecular docking computations, the docking conformation of the reference compound **WJ332** approximately agreed with the molecular dynamics simulations performed by Duque (RMSD:1.29) [15]. Two enantiomers of compound **11a** might not enter the drug-binding site cavity of M2-S31N ion channel and the direction of the molecular skeletons were almost perpendicular to the reference compound (Figure S2 in Supporting Information). As presented in Fig. **5A** and **5B**, binding modes of **WJ332**, compound**11b** and **11h** in the pore of the M2

channel drug-binding site were visualized by using UCSF Chimera [40]. Hydrophobic skeletons of the designed ligands **11b** and **11h** were located in the drug-binding sites formed by pore facing residues including Val27, Asn31 and Ala30, while the aromatic group pointed downward the C-terminus. The binding modes and orientations of the two compounds differed from those of the reference compound. In conclusion, the distinct docking results accounted for the dissimilarity between compound **11a** and pinane oxime derivatives in inhibitory activity.

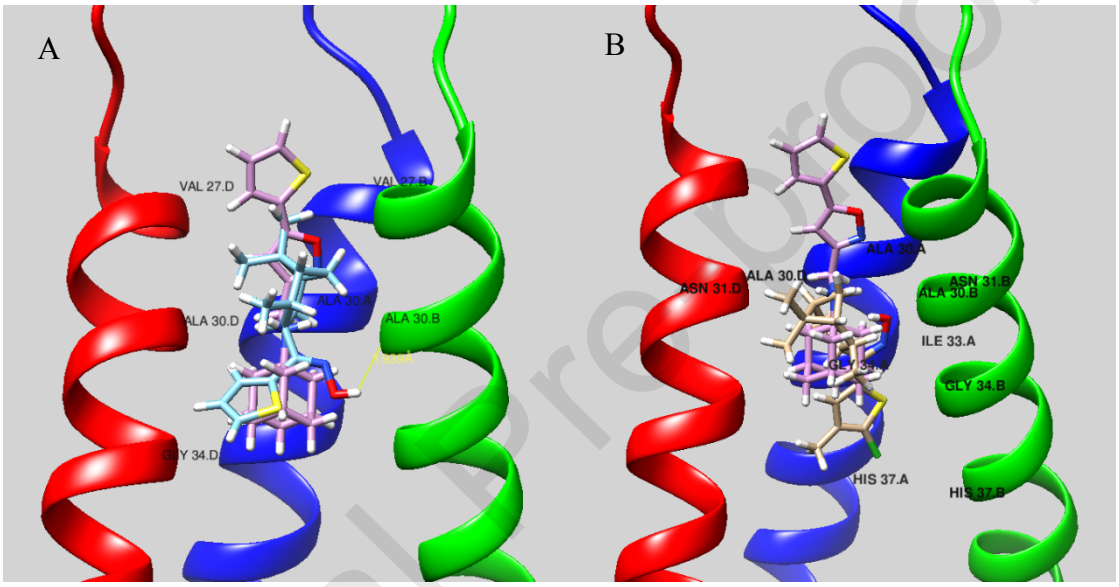

Fig. 5. A) Overlay of the reference compound **WJ332** (pink) and **11b** (sky blue) bound to M2-S31N. B) Overlay of **WJ332** (pink) and **11h** (brown) bound to M2-S31N. One helix was removed for clarity.

From Fig. **6A**, the backbone of derivative **11b** could occupy the hydrophobic region, spanning from residue Val27 to Gly30. And the thiophene moiety of **11b** formed hydrophobic interactions with the Ala30 side chains and the backbone of Gly34. In addition, the hydroxyl of oxime might form a C=O···H hydrogen bond with the carbonyl group of Ala30, with its distance being 1.939Å. These results indicated that the oxime group and the thiophene moiety had great impact on the anti-influenza activity.

Compared with compound **11b**, the most potent compound **11h** could bind more tightly to M2-S31N protein and enter the cavity created by residues Ala30, Asn31, Ile33, and Gly34, which was consistent with the results of SAR studies. Moreover, the 4-methyl-5-cholo-thiphene group proved to be crucial to enhance the binding affinity. It

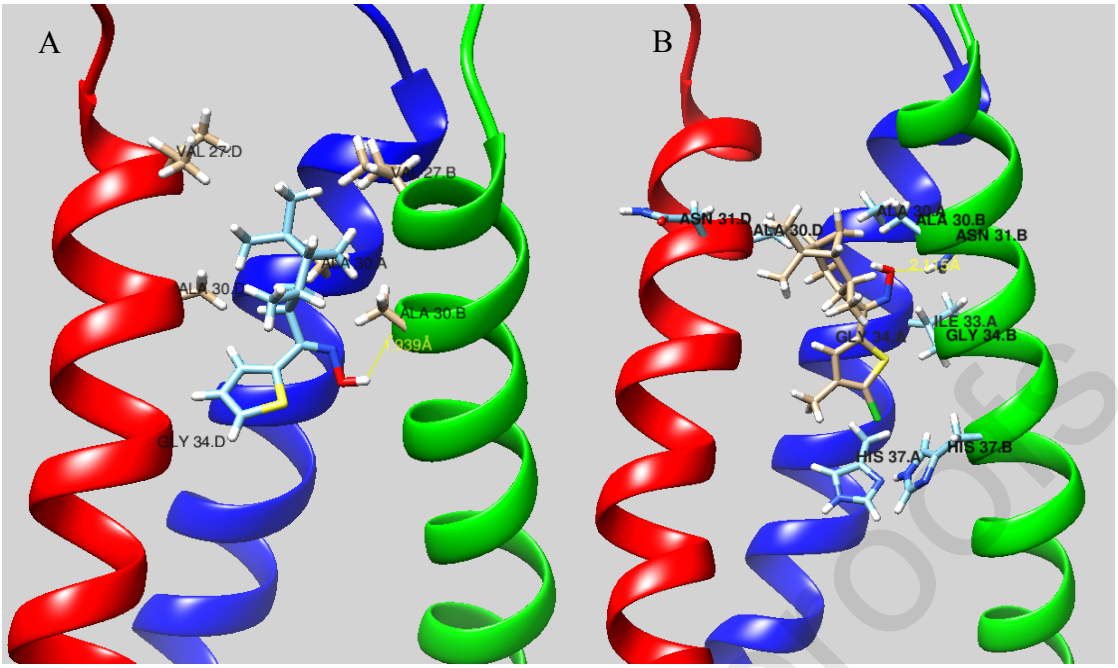

Fig. 6A-B. Docking models of compounds **11b** (sky blue) and **11h** (brown) into the drug-binding sites of M2-S31N, respectively.

seemed that the chlorine atom of compound **11h** formed a C−Cl···π halogen bond[41] with His37 side chains, which rendered the ligand to move towards the C-terminus of ion channel. Accordingly, the hydroxyl of the oxime group had a hydrogen-bonding interaction with Asn31 (OH···O=C, distance: 2.115 Å) to enhance the affinity (Fig. **6B**). To sum up, our preliminary computational analysis explained the plausible theoretical binding modes of pinane oxime derivatives, which were distinct from the reference compound. And the most potent M2-S31N antagonist **11h** could be used as a hit compound for further structural optimization.

In addition, compound **11b** and **11h** were modeled into M2 wild-type protein to clarify their binding modes, as determined by solid-state NMR (PDB code: 2KQT) [42]. Similar to amantadine, the hydrophobic backbones of the two derivatives (Fig. **7A-B**) mainly bound to the region of the channel formed mainly by Ala30 and Ser31 residues and that the polar group pointed toward the C-termini of the pore. The thiophene moiety in compound **11b** interacted with Ile33 and Gly34 *via* the hydrophobic interaction, while one hydrogen bond was formed between the ligand **11h** and the residue Ser31 (OH···O=C), with its 4-methyl-5-cholo-thiophene group facing towards the C-terminal

end. Therefore, the observed docking results provided rational explanation for the antiviral activity and the M2-WT channel inhibitory activity.

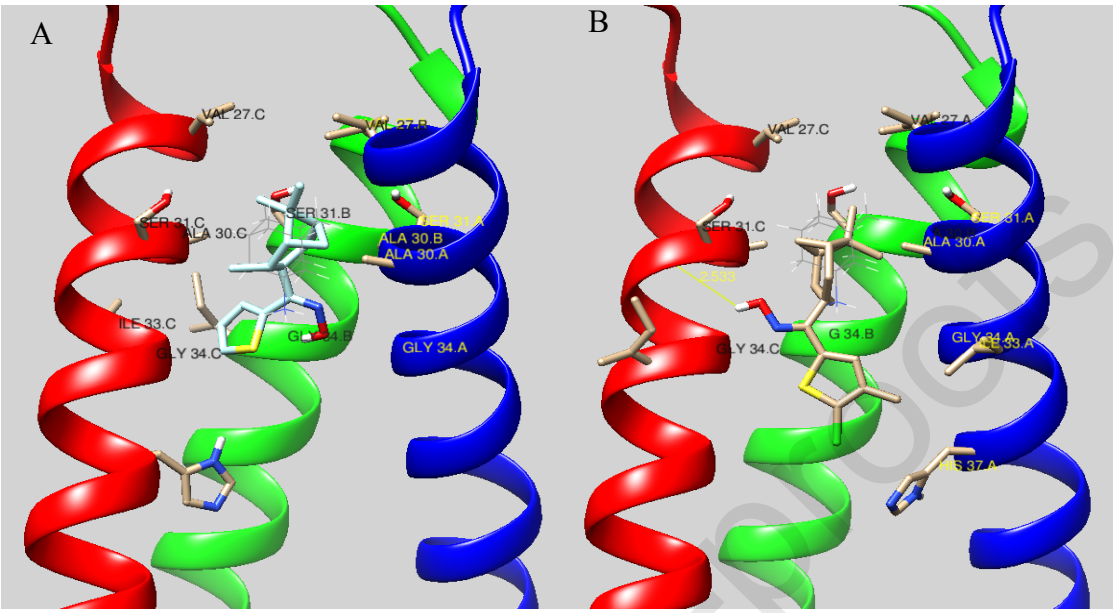

Fig. 7A-B Representation of compounds **11b** (sky blue, Fig. **7A**) and **11h** (brown, Fig. **7B**) interacting with residues in the binding site of M2-WT ion channel (PDB code: 2KQT). Amantadine was displayed as in the **wire** draw mode, with heteroatoms colored by element.

3. Conclusion

In conclusion, our study focused on the synthesis and antiviral activity studies of novel pinane oxime derivatives as M2-S31N inhibitors for anti-influenza agents to address the drug resistance. Inspired by structural characteristics of rimantadine, a series of non-adamantane-based pinane oxime derivatives were designed, synthesized and characterized by ^{1}H NMR, ^{13}C NMR, HRMS and elemental analysis. All new compounds were evaluated for their *in vitro* inhibitory activity against influenza A virus and their cytotoxicity in MDCK Cells. In light of comprehensive structure-activity relationship, the oxime group as a polar motif instead of the amine group, attached to the pinane scaffold, could maintain the antiviral activity. And the 4-methyl-5-cholo-thiophene moiety was the high-priority heterocycle for this series of compounds. In particular, compound **11h** was the most potent inhibitor against wild-type and

adamantane-resistant viruses at low micromolar concentrations through blocking M2 ion channel. Moreover, the molecular docking revealed that compound **11h** tightly bound to the pore of the drug-binding site by forming the hydrophobic interactions, halogen bonding and hydrogen bonding, with the orientation being different from the reference compound. Its antiviral efficacy *in vivo* and pharmacokinetic parameters in animal models are in progress.

4. Experimental procedure

4.1. Chemistry

Commercially available reagents were used without further purification unless otherwise noted. Reactions were monitored by TLC using Qing Dao Hai Yang GF254 silica gel plates (5×10 cm); zones were detected visually under ultraviolet irradiation (254 nm). Compounds were purified by silica gel column chromatography which performed on silica gel (200–300 mesh) from Qing Dao Hai Yang. ^{1}H NMR and ^{13}C NMR spectra were recorded on a Bruker Avance 400 spectrometer. $CDCl_3$ and DMSO-d_6 were used as solvents. Chemical shifts (δ) are given in relative to tetramethylsilane (δ 0.00 ppm) in $CDCl_3$. Coupling constants (J) were reported in hertz unit (Hz). High resolution mass spectra were performed on an Agilent 6210 LC/MSD TOF Liquid Chromatograph-ESI-Mass Spectrometer. Low-resolution mass spectra were measured on an Agilent MSD-1200 ESI-MS system. Melting points were determined using a WRS-1C melting point apparatus (Shanghai INESA Physico optiacal instrument Co. Ltd.) and were uncorrected. All final products were characterized by ^{1}H NMR, ^{13}C NMR and HRMS, selected intermediates were confirmed by ^{1}H NMR, possibly also MS. Elemental analysis was performed on an Elemental Analyzer – Elementar Vario MICRO cube.

4.1.1 *Synthesis of (1R,2R,3R,5S)-2,6,6-trimethylbicyclo[3.1.1]heptane-3-carboxylic acid 6*

A dry 500 mL single-necked rounded-bottomed flask, equipped for magnetic stirring, was charged with (-)-isopinocampheol (20.0 g, 129.66 mmol) and 200 mL dichloromethane. Pyridinium dichromate (181.5 g, 1.4 mol) was added in portions at 0 ℃ to the reaction mixture over a period of 15 min. And then the reaction mixture was stirred vigorously at room temperature until the starting material was completely consumed. The mixture was diluted with 200 mL ether and the unsolved solid was removed by filtration. The organic layer was washed with brine (200 mL), dried over anhydrous Na_2SO_4, filtered and concentrated to give the crude product. Purification by silica gel chromatography ((petroleum ether/ ethyl acetate, 50:1) yielded the desired compound (1*R*,2*R*,5*S*)-2,6,6-trimethylbicyclo[3.1.1]heptan-3-one (16.4 g, 83%) as a colorless liquid.

To an ice-cooled solution of tosylmethyl isocyanide (11.7 g, 60.00 mmol) in 40 mL dry dimethyl sulfoxide was added in portions 15.7 g of potassium tert-butylate (140.00 mmol). After stirring for 5 min, methanol (1.45 mL, 28.36 mmol) and the obtained ketone (3.0 g, 20.00 mmol) were added successively. The mixture was stirred for 48 h at 60 ℃. The reaction mixture was cooled to room temperature, diluted with 150 mL water, acidified with 2 M HCl to pH 6 and extracted with ether. The combined organic layers were washed once with saturated NaCl solution, dried and concentrated to give a brown oil. The crude product was used in the next step without further purification.

The obtained oil was dissolved in 20.0 mL AcOH, 5.0 mL H_2SO_4 and 10.0 mL H_2O, and the mixture solution was refluxed overnight. The solution was cooled to room temperature and diluted with 100 mL H_2O. The aqueous layer was extracted with dichloromethane (40 mL×3), the combined organic layers were dried over anhydrous $MgSO_4$ and concentrated *in vacuo*. The product was purified by flash column chromatography ((petroleum ether/ ethyl acetate, 40:1) to give the product (1.6g, 43.9%, over two steps) as a white powder. ^{1}H NMR (400 MHz, $CDCl_3$): δ 2.44–2.36 (m, 2H, H-3, 4β), 2.16–2.07 (m, 2H, H-2, 7β), 2.06-2.00 (m, 1H, H-2), 1.95 (q, J = 5.6 Hz, 1H,

H-5), 1.68 (t, *J* = 5.6 Hz, 1H, H-1), 1.29 (q, *J* = 10.0 Hz, 2H, H-7α, 4β), 1.21 (s, 3H, CH_3-9), 0.99 (d, *J* = 5.7 Hz, 3H, CH_3-10), 0.88 (s, 3H, CH_3-8).

4.1.2 Method A: General Procedures for Synthesizing Corresponding Weinreb Ketone 8a-j

Preparation of N-Methoxy-N-methylamide. To a 100 mL round-bottomed flask was charged with carboxyl acid **6** (1.4 g, 7.68 mmol), *N,O*-dimethylhydroxylamine hydrochloride (824.2 mg, 8.45 mmol) and acetonitrile 20 mL. 2-(1*H*-benzotriazole-1-yl)-1,1,3,3-tetramethyluronium tetrafluoroborate (TBTU) (1.87 g, 8.45 mmol) was added in portions to the reaction solution. The reaction solution was stirred at room temperature for 30min. A saturated NaCl solution was added and the product was extracted with ethyl acetate (3×50 mL). The combined organic extracts are washed with 2M HCl, H_2O, 5% $NaHCO_3$, and then brine successively, dried over $MgSO_4$, filtered, and concentrated *in vacuo* to afford the amide **7** as a yellow liquid (1.3 g, 75 %), which was purified by silica gel chromatography (petroleum ether/ethyl acetate, 15:1). ^{1}H NMR (400 MHz, $CDCl_3$): δ 3.64 (s, 3H, OCH_3), 3.20 (s, 3H, NCH_3), 3.11 (s, 1H, H-3), 1.91–1.80 (m, 2H, H-4β, 7β), 1.71–1.58 (m, 3H, H-2, 5, 1), 1.44-1.33 (m, 1H, H-7α), 1.32–1.22 (m, 1H, H-4α), 0.94 (s, 3H, CH_3-9), 0.90 (s, 3H, CH_3-10), 0.88 (s, 3H, CH_3-8). ESI-MS: calculated for $C_{13}H_{24}NO_2^+$ ($M+H^+$): 226.2, found: 226.2.

*Synthesis of thiophen-2-yl((1R,2R,3R,5S)-2,6,6-trimethylbicyclo[3.1.1]heptan-3-yl) methanone (**8a**)*. A 50 mL single-necked round-bottomed flask was charged with thiophene (0.25 mL, 3.19 mmol), and redistilled diethyl ether (5 mL), evacuated and refilled with nitrogen three times. A solution of *n*-BuLi (2.5 M in hexane, 2.98 mmol, 1.2 mL) was added dropwise to the solution at 0 ℃. The reaction mixture solution was stirred for 30 min and then cooled to -78 ℃. A solution of the Weinreb amide **7** (480 mg, 2.13 mmol) in dry diethyl ether (8 mL) was added over a period of 30 min. The reaction mixture was stirred for additional 2.5 h and quenched by 15 mL saturated ammonium chloride solution. The resulting solution was extracted with diethyl ether (3×15 mL). The combined organic layers were washed with brine (40 mL), dried over anhydrous Na_2SO_4 and evaporated *in vacuo*. The residue was purified by silica gel chromatography (petroleum ether/ ethyl acetate, 20:1) to give the Weinreb ketone **8a**

(404.0 mg, 76.3%) as a light blue liquid. ^{1}H NMR (400 MHz, $CDCl_3$): δ 7.63 (d, J = 3.6 Hz, 1H, H-5'), 7.59 (*d*, J = 5.2 Hz, 1H, H-3'), 7.10 (t, J = 4.4 Hz, 1H, H-4'), 3.60 (ddd, J = 11.2, 5.6, 2.0 Hz, 1H, H-3), 1.97–1.89 (m, 1H, H-4β), 1.82 (dd, J = 12.4, 5.2 Hz, 1H, H-7β), 1.77–1.67 (m, 2H, H-2, 5), 1.67–1.53 (m, 2H, H-1), 1.46–1.40 (m, 1H, H-7α), 1.29 (t, J = 11.2 Hz, 1H, H-4α), 1.03 (s, 3H, CH_3-9), 0.92 (s, 3H, CH_3-10), 0.90 (s, 3H, CH_3-8); ^{13}C NMR (100 MHz, $CDCl_3$) δ 195.9 (C=O), 146.8 (C-2'), 133.1 (C-5'), 131.6 (C-3'), 127.8 (C-4'), 53.1 (C-3), 51.0(C-1), 50.7 (C-5), 45.4 (C-6), 32.1 (C-2), 29.5 (C-7), 27.7 (C-4), 19.2 (C-9), 18.9 (C-8), 16.2 (C-10). ESI-MS: calculated for $C_{15}H_{21}OS^{+}$(M+H^{+}): 249.1, found: 249.1。

The following compounds were synthesized using method A: 1-((1*R*,2*R*,3*R*,5*S*)-2,6,6-trimethylbicyclo[3.1.1]heptan-3-yl)ethan-1-one (**8b**), (4-methylthiophen-2-yl)((1*R*,2*R*,3*R*,5*S*)-2,6,6-trimethylbicyclo[3.1.1]heptan-3-yl)methanone (**8c**), (3-methylthiophen-2-yl)((1*R*,2*R*,3*R*,5*S*)-2,6,6-trimethylbicyclo[3.1.1]heptan-3-yl)methanone (**8d**), (5-chloro-4-methylthiophen-2-yl)((1*R*,2*R*,3*R*,5*S*)-2,6,6-trimethylbicyclo[3.1.1]heptan-3-yl)methanone (**8e**), (5-chlorothiophen-2-yl)((1*R*,2*R*,3*R*,5*S*)-2,6,6-trimethylbicyclo[3.1.1]heptan-3-yl)methanone (**8f**), (4,5-dichlorothiophen-2-yl)((1*R*,2*R*,5*S*)-2,6,6-trimethylbicyclo[3.1.1]heptan-3-yl)methanone (**8g**), thiazol-2-yl((1*R*,2*R*,3*R*,5*S*)-2,6,6-trimethylbicyclo[3.1.1]heptan-3-yl)methanone (**8h**), (4-methoxyphenyl) ((1*R*,2*R*,3*R*,5*S*)-2,6,6-trimethylbicyclo[3.1.1]heptan-3-yl)methanone (**8i**), (4-fluorophenyl)((1*R*,2*R*,3*R*,5*S*)-2,6,6-trimethylbicyclo[3.1.1]heptan-3-yl)methanone(**8j**).

4.1.3 Method A: General Procedures for Synthesizing Corresponding Ketone 10a-d by Friede-Crafts acylation

Using the synthetic procedure of (5-bromo-4-methylthiophen-2-yl)((1*R*,2*R*,3*R*,5*S*)-2,6,6-trimethylbicyclo[3.1.1]heptan-3-yl)methanone (**10c**) as an example.

In a 100 mL round-bottomed flask equipped with a dropping funnel and a reflux condenser connected at the top to a gas absorption trap, a solution of the acid **6** (1.1 g, 6 mmol), a catalytic amount of DMF and 15 mL anhydrous CH_2Cl_2 was prepared. The resultant mixture was cooled to 0 ℃, and then thionyl chloride (1.43 g, 12.00 mmol)

was added over dropwise. The reaction solution was refluxed for 2 h. Concentration *in vacuo* offered quantitatively the crude acyl chloride **9** as a brown liquid to be used directly in the next step.

$SnCl_4$ (293 mg, 1.13 mmol) was slowly added to a mixture of acyl chloride **9** (150 mg, 0.75 mmol) and 2-bromo-3-methylthiophene (132.8 mg, 0.75 mmol) in anhydrous CH_2Cl_2 (10 mL) at 0 °C. The reaction mixture was stirred at 0 °C under nitrogen atmosphere for 1 h. TLC (petroleum ether: ethyl acetate = 10:1) indicated that the reaction was complete. The reaction mixture was quenched with 1M dilute hydrochloric acid (8 mL). The resulting solution was extracted with dichloromethane (10 mL×3). The combined organic layers were washed with brine, dried over anhydrous $MgSO_4$, filtered and concentrated. The crude product was purified by silica gel chromatography eluted with petroleum ether/ ethyl acetate (20:1) to afford the product **10c** (133 mg, 51.9%) as a yellow viscous liquid. ^{1}H NMR (400 MHz, $CDCl_3$): δ 7.39 (s, 1H, H-3'), 3.08 (q, J = 9.6 Hz, 1H, H-3), 2.66 (q, J = 7.2 Hz, 1H, H-4β), 2.23 (s, 3H, CH_3-4'), 2.19–2.10 (m, 2H, H-2, 7β), 1.98 (q, J = 5.6Hz, 1H, H-5), 1.94–1.82 (m, 1H, H-1), 1.73 (t, J = 5.6 Hz, 1H, H-7α), 1.43 (d, J = 10.0 Hz, 1H, H-4α), 1.21 (s, 3H, , CH_3-9), 0.94 (s, 3H, CH_3-8), 0.87 (d, J = 6.4 Hz, 3H, CH_3-10). ESI-MS: calculated for $C_{16}H_{22}BrOS^+$(M+H$^+$): 341.05, found: 341.1.

The following compounds were synthesized using method B: (5-methylthiophen-2-yl)((1R,2R,5S)-2,6,6-trimethylbicyclo[3.1.1]heptan-3-yl)methanone (**10a**), (4,5-dimethylthiophen-2-yl)((1R,2R,5S)-2,6,6-trimethylbicyclo[3.1.1]heptan-3-yl)methanone (**10b**), (5-methoxythiophen-2-yl)((1R,2R,5S)-2,6,6-trimethylbicyclo[3.1.1]heptan-3-yl) methanone (**10d**).

4.1.4 Synthesis of thiophen-2-yl((1R,2R,3R,5S)-2,6,6-trimethylbicyclo[3.1.1]heptan-3-yl)methanamine·HCl (11a)

A 25 mL round bottom flask was charged with compound **8a** (372 mg, 1.5 mmol), methoxyamine hydrochloride (250.6 mg, 3 mmol) and pyridine 10 mL. The reaction mixture was stirred at 80 ℃ for 24 h. After azeotropic removal of solvent by evaporation

with n-hexane, the residue was partitioned between 50 mL dichloromethane (50 mL) and brine (50 mL). The separated organic layer was dried over anhydrous Na_2SO_4, filtered, and concentrated *in vacuo*. The crude product was purified by column chromatography (petroleum ether/ ethyl acetate, 100:1) to give O-methyl oxime derivative **12** (220 mg, 52.8%) as a yellow oil. ^{1}H NMR (400 MHz, $CDCl_3$): δ 7.57 (d, J = 5.0 Hz, 1H), 7.33 (d, J = 3.5 Hz, 1H), 7.06 (t, J = 4.4 Hz, 1H), 2.97–2.64 (m, 2H, H-3, 4β), 2.28 (s, 3H, OCH_3), 2.24–2.17 (m, 2H, H-2, 7β), 2.15–2.09 (m, 1H, H-5), 1.95 (q, J = 5.6 Hz, 1H, H-1), 1.78 (d, J = 5.6 Hz, 1H, H-7α), 1.73 (t, J = 10.0 Hz, 1H, H-4α), 1.22 (s, 3H, , CH_3-9), 0.95 (s, 3H, CH_3-8), 0.88 (d, J = 6.4 Hz, 3H, CH_3-10). ESI-MS: calculated for $C_{17}H_{26}NOS^+$(M+H$^+$): 292.17, found: 292.2.

To a solution of obtained oxime ester **12** (220 mg, 0.79 mmol) in 15 mL dry ether was added dropwise a solution of (1.58 mL, 5 equiv.) 2.4 M lithium aluminum hydride solution in tetrahydrofuran under argon atmosphere at 0 ℃. The resulting suspension was stirred at 40 ℃ for 4 h. After the reaction mixture was cooled to 0 ℃, moist Na_2SO_4 solid was added slowly, and the resulting precipitate was removed by Celite filtration and washed by THF several times. The combined filtrates were concentrated to dryness and the residue was purified by silica gel chromatography using petroleum ether/ethyl acetate (5:1) as an eluent to afford the free amine (60 mg, 30.4 %) as a light yellow liquid. Corresponding salt **11a** was prepared by addition of saturated hydrogen chloride in ethyl acetate solution. White solid, m.p. 216.3–217.6 ℃. ^{1}H NMR (400 MHz, DMSO-d_6): δ 8.68 (m, 3H, -NH_3^+), 7.58 (d, J = 4.8 Hz, 1H, H-5'), 7.40 (d, J = 2.4 Hz, 1H, H-3'), 7.08 (t, J = 4.0 Hz, 1H, H-4'), 4.50-4.46 (m, 1H, N-CH), 2.05–1.96 (m, 2H, H-3, 4β), 1.94–1.88 (m, 2H, H-7β, 2), 1.83–1.70 (m, 2H, H-1, 5), 1.52 (t, J = 5.6 Hz, 1H, H-7α), 1.22 (s, 1H, H-4α), 1.16 (s, 3H, CH_3-9), 0.80 (s, 3H, CH_3-8), 0.24 (d, J = 6.4 Hz, 3H, CH_3-10); ^{13}C NMR (100 MHz, DMSO-d_6): δ 141.0 (C-2'), 127.7(C-5'), 127.6 (C-3'), 126.8 (C-4'), 55.1(N-*C*H), 48.7(C-3), 41.1(C-1), 40.1(C-5), 39.3(C-6), 33.6(C-2), 29.2(C-7), 26.9(C-4), 24.1(C-9), 20.7 (C-8), 20.5(C-10). HRMS calcd for $C_{15}H_{24}NS^+$(M+H$^+$), 250.1624; found, 250.1619. Anal. Calcd. (%) for $C_{15}H_{24}ClNS$: C, 63.02; H, 8.46; N, 4.90; Found: C, 62.94; H, 8.49; N, 5.3.

4.1.5 General Procedures for Synthesizing Pinane Oxime Derivatives 11b-o.

Using the synthetic procedure of (E)-(5-chloro-4-methylthiophen-2-yl)((1R,2R,3R,5S) -2,6,6-trimethylbicyclo[3.1.1]heptan-3-yl)methanone oxime ***(11h)*** *as an example.*

A 25 mL round bottom flask was charged with the corresponding ketone **8e** (430 mg, 1.44 mmol), hydroxylamine hydrochloride (300 mg, 4.32 mmol) and pyridine 10 mL. The reaction mixture was stirred at 80 ℃ for 24 h. After azeotropic removal of solvent by evaporation with n-hexane, the residue was partitioned between dichloromethane and water. The separated organic layer was washed with brine, dried over anhydrous Na_2SO_4 and evaporated to dryness. The crude product was purified by silica gel chromatography to give single ant-isomer **11h** (247 mg, 55.01 %) as a white solid. m.p. 168.4–170.1 ℃. ^{1}H NMR (400 MHz, DMSO-*d6*): δ 12.00 (s, 1H, -O*H*), 7.50 (s, 1H, H-3'), 2.98 (q, J = 9.6 Hz, 1H, H-3), 2.71 (q, J = 7.2 Hz, 1H, H-4β), 2.26–2.20 (m, 1H, H-7β), 2.18 (s, 3H, Ar-CH_3), 2.13–2.03 (m, 1H, H-2), 1.92 (q, J = 5.6 Hz, 1H, H-5), 1.70–1.67 (m, 2H, H-1, 7α), 1.64–1.55 (m, 1H, H-4α), 1.20 (s, 3H, CH_3-9), 0.91 (s, 3H, CH_3-8), 0.82 (d, J = 6.4 Hz, 3H, CH_3-10)； ^{13}C NMR (100 MHz, DMSO-d_6): δ 150.8 (C=N), 133.0 (C-4'), 130.5(C-5'), 128.8 (C-2'), 128.6 (C-3'), 47.2 (C-3), 40.9 (C-1), 40.2 (C-5), 38.82 (C-6), 32.9 (C-2), 32.6 (C-7), 27.1 (C-4), 23.2 (C-9), 20.5 (C-8), 20.4 (C-10), 13.5 (Ar-C). HRMS calcd for $C_{16}H_{23}ClNOS^+$(M+H$^+$): 312.1183, found: 312.1188. Anal. Calcd. (%) for $C_{16}H_{22}ClNOS$: C, 61.62; H, 7.11; N, 4.49; Found: C, 61.56; H, 7.07; N, 4.44.

4.1.5.1. (thiophen-2-yl)((1R,2R,3R,5S)-2,6,6-trimethylbicyclo[3.1.1]heptan-3-yl)methanone oxime ***(11b)***. Pale yellow solid, yield: 62.8%, m.p. 159.6–161.2 ℃. ^{1}H NMR (400 MHz, $CDCl_3$): δ 9.10 (s, 1H, -O*H*), 7.52–7.50 (m, 2H, H-3', 5'), 7.08 (t, J = 4.4 Hz, 1H, H-4'), 3.46–3.42 (m, 1H, H-3), 2.10–2.02 (m, 1H, H-4β), 1.95–1.89 (m, 1H, H-7β), 1.80–1.70 (m, 3H, H-2, 5, 1), 1.40–1.22 (m, 2H, H-4α,7α), 1.04 (s, 3H, Me-9), 0.92 (s, 3H, Me-10), 0.70 (s, 3H, Me-8). ^{13}C NMR (100 MHz, DMSO-d_6): δ 156.0 (C=N), 142.4 (C-2'), 141.6 (C-5'), 127.6 (C-3'), 121.6 (C-4'), 47.5 (C-3), 46.8 (C-1), 41.3 (C-5), 34.3 (C-6), 33.1 (C-2), 31.4 (C-7), 28.9 (C-4), 26.8 (C-9), 19.6 (C-8), 19.5

(C-10). HRMS calcd for $C_{15}H_{22}NOS+$ ($M+H^+$): 264.1417, found: 264.1421. Anal. Calcd. (%) for $C_{15}H_{21}NOS$: C, 68.40; H, 8.04; N, 5.32; Found: C, 68.51; H, 7.99; N, 5.22.

*4.1.5.2. 1-((1R,2R,3R,5S)-2,6,6-trimethylbicyclo[3.1.1]heptan-3-yl)ethan-1-one oxime (**11c**)*. White solid, yield: 70.3%, m.p. 140.2–141.9 ℃. ^{1}H NMR (400 MHz, DMSO-d_6): δ 10.34 (s, 1H, -O*H*), 2.38 (p, J = 7.2 Hz, 1H, H-3), 2.20 (q, J = 9.6 Hz, 1H, H-4β), 2.07–1.88 (m, 3H, H-7β, 5, 2), 1.79 (s, 3H, N=C-CH_3), 1.65–1.56 (m, 2H, H-1, 7α), 1.42 (d, J = 10.0 Hz, 1H, 4α), 1.18 (s, 3H, CH_3-9), 0.81 (s, 3H, CH_3-8), 0.80 (d, J = 6.4 Hz, 3H, CH_3-10); ^{13}C NMR (100 MHz, DMSO-d_6): δ 157.2 (C=N), 47.1 (C-3), 42.4 (C-1), 40.6 (C-5), 40.0 (C-6), 30.9 (C-2), 29.9 (C-7), 27.1 (C-4), 23.3 (C-9), 20.4 (C-8), 20.1 (C-10), 13.3 (N=C-*C*H$_3$). HRMS calcd for $C_{12}H_{22}NO^+$ ($M+H^+$): 196.1696, found: 196.1700. Anal. Calcd. (%) for $C_{12}H_{21}NO$: C, 73.80; H, 10.84; N, 7.17; Found: C, 73.86; H, 10.78; N, 7.05.

*4.1.5.3. (4-methylthiophen-2-yl)((1R,2R,3R,5S)-2,6,6-trimethylbicyclo[3.1.1]heptan-3-yl)methanone oxime (**11d**)*. Light yellow solid, yield: 68.4%, m.p. 177.7–180.1 ℃. ^{1}H NMR (400 MHz, DMSO-d_6): δ 11.64 (s, 1H, -O*H*), 7.46 (s, 1H, H-5'), 7.28 (s, 1H H-3'), 2.97 (q, J = 9.6 Hz, 1H, H-3), 2.77–2.69 (m, 1H, H-4β), 2.26–2.19 (m, 4H, CH_3-4', 7β), 2.09–2.07 (m, 1H, H-2), 1.92 (q, J = 5.6 Hz, 1H, H-5), 1.72–1.55 (m, 3H, H-1, 7α, 4α), 1.20 (s, 3H, CH_3-9), 0.91 (s, 3H, CH_3-8), 0.82 (d, J = 6.4 Hz, 3H, CH_3-10); ^{13}C NMR (100 MHz, DMSO-d_6): δ 150.6 (C=N), 135.5 (C-4'), 132.8 (C-2'), 130.7 (C-5'), 125.6 (C-3'), 47.3 (C-3), 40.8 (C-1), 32.6 (C-5), 32.5 (C-6,C-2), 26.7 (C-7), 22.9 (C-4), 20.2(C-8, C-9), 20.0 (C-10), 15.2 (Ar-*C*H$_3$). HRMS calcd for $C_{16}H_{24}NOS^+$($M+H^+$): 278.1573, found: 278.1569. Anal. Calcd. (%) for $C_{16}H_{23}NOS$: C, 69.27; H, 8.36; N, 5.05; Found: C, 69.23; H, 8.32; N, 5.11.

*4.1.5.4. (3-methylthiophen-2-yl)((1R,2R,3R,5S)-2,6,6-trimethylbicyclo[3.1.1]heptan-3-yl) methanone oxime (**11e**)*. Light yellow solid, yield: 64.9%, m.p. 174.8–176.4 ℃. ^{1}H NMR (400 MHz, DMSO-d_6): δ 10.94 (s, 1H, -O*H*), 7.50 (d, J = 5.0 Hz, 1H, H-5'), 6.91 (d, J = 5.0 Hz, 1H, H-4'), 2.48–2.44 (m, 1H, H-3), 2.07 (s, 3H, Ar-CH_3), 2.04–2.01 (m, 1H, H-4β), 1.92–1.79 (m, 2H, H-2, 7β), 1.75–1.70 (m, 1H, H-5), 1.64 (t, J =

5.6 Hz, 1H, H-1), 1.41 (d, *J* = 10.0 Hz, 1H, H-7α),1.30-1.21 (m, 1H, H-4α) 1.16 (s, 3H, C*H*$_3$-9), 0.87 (d, *J* = 5.6 Hz, 3H, C*H*$_3$-10), 0.72 (s, 3H, C*H*$_3$-8). ^{13}C NMR (100 MHz, DMSO-*d*$_6$): *δ* 142.7 (C=N), 135.9 (C-3'), 129.9 (C-2'), 128.7 (C-4'), 126.3(C-5'), 47.3 (C-3), 44.7 (C-1), 40.5 (C-5), 39.7 (C-6), 32.0 (C-2), 30.0 (C-7), 26.9 (C-4), 23.2 (C-9), 20.1 (C-8), 19.5 (C-10), 14.5 (Ar-*C*H$_3$). HRMS calcd for $C_{16}H_{24}NOS^+$(M+H$^+$): 278.1573, found: 278.1571. Anal. Calcd. (%) for $C_{16}H_{23}NOS$: C, 69.27; H, 8.36; N, 5.05; Found: C, 69.30; H, 8.41; N, 5.02.

*4.1.5.5. (5-methylthiophen-2-yl)((1R,2R,3R,5S)-2,6,6-trimethylbicyclo[3.1.1]heptan-3-yl)methanone oxime (**11f**)*. Light yellow solid, yield: 71.9%, m.p. 175.2–176.7 ℃. ^{1}H NMR (400 MHz, $CDCl_3$): *δ* 8.25 (s, 1H, -O*H*), 7.37 (s, 1H, H-3'), 6.77 (s, 1H, H-4'), 2.95–2.87 (m, 1H, H-3), 2.70 (s, 1H, H-4β), 2.52 (s, 3H, Ar-C*H*$_3$), 2.21 (s, 1H, H-7β), 2.13 (s, 1H, H-2), 1.96 (s, 1H, H-5), 1.82–1.76 (m, 2H, H-1), 1.58–1.52 (m, 2H, H-7α, 4α), 1.24 (s, 3H, C*H*$_3$-9), 0.94 (s, 3H, C*H*$_3$-8), 0.90 (d, *J* = 6.4 Hz, 3H, C*H*$_3$-10); ^{13}C NMR (100 MHz, $CDCl_3$): *δ* 153.7 (C=N), 144.8 (C-2'), 131.5 (C-5'), 130.1 (C-4'), 124.7 (C-3'), 48.3 (C-3), 41.8 (C-1), 41.7 (C-5), 40.7 (C-6), 33.2 (C-2), 33.1 (C-7), 27.4 (C-4), 23.8 (C-9), 20.6 (C-8), 20.4 (C-10), 15.3 (Ar-*C*H$_3$). HRMS calcd for $C_{16}H_{24}NOS^+$(M+H$^+$): 278.1573, found: 278.1578. Anal. Calcd. (%) for $C_{16}H_{23}NOS$: C, 69.27; H, 8.36; N, 5.05; Found: C, 69.22; H, 8.29; N, 5.10.

*4.1.5.6. (4,5-dimethylthiophen-2-yl)((1R,2R,3R,5S)-2,6,6-trimethylbicyclo[3.1.1]heptan-3-yl)methanone oxime (**11g**)*. White solid, yield: 63.2%, m.p. 189.1–190.4 ℃. ^{1}H NMR (400 MHz, DMSO-*d*$_6$): *δ* 11.47 (s, 1H, -O*H*), 7.34 (s, 1H, H-3'), 2.93 (q, *J* = 9.6 Hz, 1H, H-3), 2.71 (s, 1H, H-4β), 2.29 (s, 3H, C*H*$_3$-5'), 2.23–2.16 (m, 1H, H-7β), 2.11 (s, 3H, C*H*$_3$-4'), 2.07 (s, 1H, H-2), 1.91 (d, *J* = 5.7 Hz, 1H, H-5), 1.69–1.57 (m, 3H, H-1, 7α, 4α), 1.20 (s, 3H, C*H*$_3$-9), 0.91 (s, 3H C*H*$_3$-8), 0.81 (d, *J* = 6.4 Hz, 3H, C*H*$_3$-10); ^{13}C NMR(100 MHz, $CDCl_3$): *δ* 153.6 (C=N), 138.4 (C-5'), 132.9 (C-2'), 132.7 (C-4'), 129.0 (C-3'), 48.3 (C-3), 41.8 (C-1), 41.7 (C-5), 40.8 (C-6), 33.3 (C-2), 33.1 (C-7), 27.4 (C-4), 23.8 (C-9), 20.6 (C-8), 20.4 (C-10), 13.8 (Ar-*C*H$_3$-4'), 13.2 (Ar-*C*H$_3$-5'). HRMS calcd for $C_{17}H_{26}NOS^+$(M+H$^+$): 292.1730, found: 292.1736. Anal. Calcd. (%) for $C_{17}H_{25}NOS$: C, 70.06; H, 8.65; N, 4.81; Found: C, 70.00; H, 8.59; N, 4.91.

4.1.5.7. (5-bromo-4-methylthiophen-2-yl)((1R,2R,3R,5S)-2,6,6-trimethylbicyclo[3.1.1]

*heptan-3-yl)methanone oxime (**11i**)*. White solid, yield: 66.6%, m.p. 165.4–167.1 ℃. ^{1}H NMR (400 MHz, DMSO-d_6): δ 11.98 (s, 1H, -O*H*), 7.47 (s, 1H, H-3'), 2.97 (q, J = 9.6 Hz, 1H, H-3), 2.71 (p, J = 7.2 Hz, 1H, H-4β), 2.25–2.21 (m, 1H, H-7β), 2.18 (s, 3H, Ar-CH_3), 2.11–2.05 (m, 1H, H-2), 1.91 (q, J = 5.6 Hz, 1H, H-5), 1.70–1.66 (m, 2H, H-1, 7α), 1.64–1.52 (m, 1H, H-4α), 1.20 (s, 3H, CH_3-9), 0.90 (s, 3H, CH_3-8), 0.81 (d, J = 6.4 Hz, 3H, CH_3-10); ^{13}C NMR (100 MHz, DMSO-d_6): δ 150.8 (C=N), 135.7 (C-4'), 131.9 (C-5'), 130.6 (C-2'), 115.2 (C-3'), 55.3 (C-3), 47.2 (C-1), 40.9 (C-5), 38.9 (C-6), 32.9 (C-2), 32.6 (C-7), 27.1 (C-4), 23.2 (C-9), 20.5 (C-8), 20.4 (C-10), 15.1 (Ar-C). HRMS calcd for $C_{16}H_{23}BrNOS^+$(M+H$^+$): 356.0678, found: 356.0680. Anal. Calcd. (%) for $C_{16}H_{22}BrNOS$: C, 53.93; H, 6.22; N, 3.93; Found: C, 53.88; H, 6.20; N, 4.01.

*4.1.5.8. (5-chlorothiophen-2-yl)((1R,2R,3R,5S)-2,6,6-trimethylbicyclo[3.1.1]heptan-3-yl) methanone oxime (**11j**)*. White solid, yield: 56.1%, m.p. 170.8–172.2 ℃. ^{1}H NMR (400 MHz, DMSO-d_6): δ 12.09 (s, 1H, -O*H*), 7.54 (d, J = 4.0 Hz, 1H, H-3'), 7.15 (d, J = 4.0 Hz, 1H, H-4'), 3.00 (q, J = 9.6 Hz, 1H, H-3), 2.70 (p, J = 7.2, 1H, H-4β), 2.22–2.16 (m, 1H, H-7β), 2.09–2.06 (m, 1H, H-2), 1.94–1.88 (m, 1H, H-5), 1.71–1.57 (m, 3H, H-1, 7α, 4α)), 1.20 (s, 3H, CH_3-9), 0.90 (s, 3H, CH_3-8), 0.81 (d, J = 6.4 Hz, 3H, CH_3-10); ^{13}C NMR (100 MHz, DMSO-d_6): δ 160.0 (C=N), 132.1 (C-2'), 130.2 (C-5'), 127.7 (C-4'), 124.6 (C-3'), 46.3 (C-3), 39.0 (C-1), 38.8 (C-5), 37.8 (C-6), 31.9 (C-2), 31.8 (C-7), 26.1(C-4), 22.2(C-9), 19.6(C-8), 19.4(C-10). HRMS calcd for $C_{15}H_{21}ClNOS^+$ (M+H$^+$): 298.1027, found: 298.1034. Anal. Calcd. (%) for $C_{15}H_{20}ClNOS$: C, 60.49; H, 6.77; N, 4.70; Found: C, 60.43; H, 6.72; N, 4.76.

*4.1.5.9. (4,5-dichlorothiophen-2-yl)((1R,2R,3R,5S)-2,6,6-trimethylbicyclo[3.1.1]heptan-3-yl)methanone oxime (**11k**)*. White solid, yield: 79.7%, m.p. 186.4–187.9 ℃. ^{1}H NMR (400 MHz, DMSO-d_6): δ 12.42 (s, 1H, -O*H*), 7.76 (s, 1H, H-3'), 3.02 (q, J = 9.6 Hz, 1H, H-3), 2.69 (t, J = 7.2 Hz, 1H, H-4β), 2.24–2.14 (m, 1H, H-7β), 2.07–2.03 (m, 1H, H-2), 1.93–1.88 (m, 1H, H-5), 1.73 (d, J = 10.0 Hz, 1H, H-1), 1.68 (d, J = 5.6 Hz, 1H, H-7α), 1.64–1.53 (m, 1H, H-4α), 1.20 (s, 3H, CH_3-9), 0.90 (s, 3H, CH_3-8), 0.82 (d, J = 6.4 Hz, 3H, CH_3-10); ^{13}C NMR (100 MHz, DMSO-d_6): δ 143.9 (C=N), 132.4 (C-2'), 130.0 (C-5'), 127.0 (C-4'), 121.6 (C-3'), 56.1 (C-3), 47.5 (C-1), 40.8 (C-5), 40.6 (C-6), 38.8 (C-2), 32.3 (C-7), 31.2 (C-4), 27.7 (C-9), 23. 8 (C-8), 21.2 (C-10). HRMS

calcd for $C_{15}H_{20}Cl_2NOS$ ($M+H^+$): 332.0637, found: 332.0642. Anal. Calcd. (%) for $C_{15}H_{19}Cl_2NOS$: C, 54.22; H, 5.76; N, 4.22; Found: C, 54.18; H, 5.78; N, 4.19.

*4.1.5.10. (5-methoxythiophen-2-yl)((1R,2R,3R,5S)-2,6,6-trimethylbicyclo[3.1.1]heptan-3-yl)methanone oxime(**11l**)*. Yellow solid, yield: 65.1%, m.p. 154.6–155.9 ℃. ^{1}H NMR (400 MHz, DMSO-d_6): δ 11.46 (s, 1H, -O*H*), 7.32 (d, J = 4.4 Hz, 1H, H-3'), 6.32 (d, J = 4.4 Hz, 1H, H-4'), 3.88 (s, 3H, OCH_3), 2.94 (t, J = 9.6 Hz, 1H, H-3), 2.73–2.66 (m, 1H, H-4β), 2.20–2.14 (m, 1H, H-7β), 2.11–2.02 (m, 1H, H-2), 1.90 (d, J = 6.0 Hz, 1H, H-5), 1.69–1.59 (m, 3H, H-1, 7α, 4α), 1.20 (s, 3H, CH_3-9), 0.92 (s, 3H, CH_3-8), 0.81 (d, J = 6.4 Hz, 3H, CH_3-10); ^{13}C NMR (100 MHz, DMSO-d_6): δ 169.7 (C=N), 151.3 (C-5'), 127.8 (C-2'), 118.8 (C-3'), 103.0 (C-4'), 60.1 (OCH_3), 47.3 (C-3), 40.9 (C-1), 38.7 (C-5), 33.1 (C-6), 32.7 (C-2), 27.1 (C-7), 23.2 (C-4), 20.6 (C-8, C-9), 20.4 (C-10). HRMS calcd for $C_{16}H_{24}Cl_2NO_2S^+$($M+H^+$): 294.1522, found: 294.1525. Anal. Calcd. (%) for $C_{16}H_{23}$NO2S: C, 65.49; H, 7.90; N, 4.77; Found: C, 65.41; H, 7.96; N, 4.75.

*4.1.5.11. thiazol-2-yl((1R,2R,3R,5S)-2,6,6-trimethylbicyclo[3.1.1]heptan-3-yl)methanone oxime (**11m**)*. Pale yellow solid, yield: 70.2%, m.p. 170.5–172.4 ℃. ^{1}H NMR(400 MHz, DMSO-d_6): δ 12.54 (s, 1H, -O*H*), 8.03 (d, J = 3.2 Hz, 1H, H-5'), 7.96 (d, J = 3.2 Hz, 1H, H-4'), 3.54 (q, J = 9.6 Hz, 1H, H-3), 2.74–2.67 (m, 1H, H-4β), 2.35–2.28 (m, 1H, H-7β), 2.14–2.09 (m, 1H, H-2), 1.93 (q, J = 5.0 Hz, 1H, H-5), 1.71 (t, J = 5.6 Hz, 1H, H-1), 1.62–1.54 (m, 2H, H-7α, 4α), 1.21 (s, 3H, CH_3-9), 0.93 (s, 3H, CH_3-8), 0.81 (d, J = 6.4 Hz, 3H, CH_3-10); ^{13}C NMR (100 MHz, DMSO-d_6): δ 155.1 (C=N), 152.1 (C-2'), 142.0 (C-4'), 124.3 (C-5'), 47.3 (C-3), 40.9 (C-1), 40.2 (C-5), 38.7 (C-6), 32.5 (C-2), 32.4 (C-7), 27.1 (C-4), 23.4 (C-8), 20.5 (C-9), 20.3(C-10). HRMS calcd for $C_{14}H_{21}N_2OS^+$($M+H^+$): 265.1369, found: 265.1372. Anal. Calcd. (%) for $C_{14}H_{20}N_2OS$: C, 63.60; H, 7.63; N, 10.60; Found: C, 63.55; H, 7.65; N, 10.58.

*4.1.5.12. (4-methoxyphenyl)((1R,2R,3R,5S)-2,6,6-trimethylbicyclo[3.1.1]heptan-3-yl) methanone oxime (**11n**)*. Pale yellow solid, yield: 53.5%, m.p. 194.3–196.1 ℃. ^{1}H NMR (400 MHz, DMSO-d_6) δ 10.46 (s, 1H, -O*H*), 7.25 (d, J = 8.0 Hz, 2H, H-2', 6'), 6.93 (d, J = 8.0 Hz, 2H, H-3', 5'), 3.76 (s, 3H, OCH_3), 2.57 (q, J = 9.6 Hz, 1H, H-3), 2.48–2.44 (m, 1H, H-4β), 2.04–2.00 (m, 1H, H-7β), 1.90–1.72 (m, 2H, H-2, 5), 1.71–1.57 (m, 2H,

H-1, 7α), 1.44 (d, J = 10.0 Hz, 1H, H-4α), 1.16 (s, 3H, CH_3-9), 0.86 (d, J = 6.4 Hz, 3H, CH_3-10), 0.72 (s, 3H, CH_3-8); ^{13}C NMR (100 MHz, DMSO-d_6) δ 159.1 (C=N), 158.0 (C-4'), 129.6 (C-2', C-6'), 127.9 (C-1'), 113.6 (C-3', C-5'), 55.4 (O*C*H$_3$), 47.3 (C-3), 42.1 (C-1), 40.6 (C-5), 31.9 (C-6), 30.9 (C-2), 27.0 (C-7), 23.4 (C-4), 20.4 (C-8, C-9), 20.1 (C-10). HRMS calcd for $C_{18}H_{26}NO_2^+$ (M+H$^+$): 288.1958, found: 288.1960. Anal. Calcd. (%) for $C_{18}H_{25}NO_2$: C, 75.22; H, 8.77; N, 4.87; Found: C, 75.28; H, 8.82; N, 4.83.

*4.1.5.13. (4-fluorophenyl)((1R,2R,3R,5S)-2,6,6-trimethylbicyclo[3.1.1]heptan-3-yl) methanone oxime (**11o**)*. White solid, yield: 72.6%, m.p. 190.5–191.1 ℃. ^{1}H NMR (400 MHz, DMSO-d_6): δ 10.63 (s, 1H, -O*H*), 7.33 (t, J = 7.6 Hz, 2H, H-2', 6'), 7.22 (t, J = 8.8 Hz, 2H, H-3', 5'), 2.57 (q, J = 9.6 Hz, 1H, H-3), 2.45 (t, J = 7.2 Hz, 1H, H-4β), 2.05–2.00 (m, 1H, H-7β), 1.86 (q, J = 5.6 Hz, 1H, H-2), 1.80–1.73 (m, 1H, H-5), 1.70–1.62 (m, 2H, H-1, 7α), 1.44 (d, J = 10.0 Hz, 1H, H-4α), 1.15 (s, 3H, CH_3-9), 0.87 (d, J = 6.4 Hz, 3H, CH_3-10), 0.69 (s, 3H, CH_3-8); ^{13}C NMR (100 MHz, DMSO-d_6): δ 161.9 (d, $^1J_{CF}$ = 242.8 Hz, C-4'),157.8 (C=N), 132.0 (C-1'), 130.4 (d, $^3J_{CF}$ = 8.1 Hz, C-2', C-6'), 115.2 (d, $^2J_{CF}$ = 21.3 Hz, C-3', C-5'), 47.2 (C-3), 42.1 (C-1), 40.5 (C-5), 31.8(C-6), 30.6 (C-2), 27.0 (C-7), 23.3 (C-4), 20.4 (C-8, C-9), 20.0 (C-10). HRMS calcd for $C_{17}H_{23}FNO^+$(M+H$^+$): 276.1758, found: 276.1755. Anal. Calcd. (%) for $C_{17}H_{22}FNO$: C, 74.15; H, 8.05; N, 5.09; Found: C, 74.12; H, 8.01; N, 5.13.

4.1.6 Synthesis of Compound 14a and 14b

A solution of compound **11d** (50 mg, 0.18 mmol) in 5 mL anhydrous DMF was treated with 60% sodium hydride (18 mg, 0.45 mmol) at 0 ℃ and stirred for 1 h. Then tert-butyl (*S*)-2-(bromomethyl)pyrrolidine-1-carboxylate (57 mg, 0.22 mmol) was added in portions. The reaction mixture was stirred at room temperature for 4 h, quenched by adding saturated $NaHCO_3$ solution (8 mL), and then extracted with ethyl acetate (3×10 mL). The combined organic layers were washed with brine (15 mL), dried, filtered, and concentrated under reduced pressure. The crude residue was purified by column chromatography (petroleum ether/ethyl acetate, 50:1) to give a colorless oil.

The product was dissolved in ethyl acetate (2 mL) and treated with excess saturated hydrogen chloride in ethyl acetate solution. Upon removal of the solvent, the residue was triturated with ether, filtered and dried to afford compound **14a** as a white solid (55 mg, 76.9%). m.p. 210.2–212.0 ℃. ^{1}H NMR (400 MHz, DMSO-d_6): δ 9.62 (s, 1H, pyrrolidine-N*H*), 9.05 (s, 1H s, pyrrolidine-N*H*), 7.62 (s, 1H, H-5'), 7.42 (s, 1H, H-3'), 4.65 – 4.13 (m, 2H, -OCH_2-), 3.84 (s, 1H, NC*H*), 3.19 (s, 2H, pyrrolidine-NCH_2), 3.01 (q, J = 9.6 Hz, 1H, H-3), 2.71–2.67 (m, 1H, H-4β), 2.25 (s, 3H, Ar-CH_3), 2.21-2.18 (m, 1H, H-7β), 2.09 (s, 2H, pyrrolidine-NCH$_2$CH_2), 2.01–1.82 (m, 3H, H-2, 5, 1), 1.81–1.71 (m, 1H, H-7α), 1.72–1.59 (m, 3H, pyrrolidine-NCHCH_2, H-4α), 1.20 (s, 3H, CH_3-9), 0.91 (s, 3H, CH_3-8), 0.83 (d, J = 6.4 Hz, 3H, CH_3-10). ^{13}C NMR (100 MHz, DMSO-d_6): δ 153.2 (C=N), 136.6 (C-4'), 133.1 (C-2'), 132.3 (C-5'), 127.4 (C-3'), 73.3 (O*C*H$_2$), 58.1 (pyrrolidine-C-2''), 47.3 (C-3), 45.6 (pyrrolidine-C-5''), 40.9 (C-1), 40.3 (C-5), 33.0 (C-6), 32.7 (C-2), 27.4 (pyrrolidine-C-3'') , 27.2 (C-7), 23.6 (pyrrolidine-C-4''), 23.2 (C-4), 20.6 (C-8, C-9), 20.2 (C-10), 15.6 (Ar-C). HRMS calcd for $C_{21}H_{33}N_2OS^+$(M+H$^+$): 361.2308, found: 361.2306. Anal. Calcd. (%) for $C_{21}H_{33}ClN_2OS$: C, 63.53; H, 8.38; N, 7.06; Found: C, 63.48; H, 8.36; N, 7.10.

Compound **14b** (48 mg, 71.2%) as a yellow solid **was** prepared from compound **11d** (50 mg, 0.18 mmol), 2-pyrrolidinoethyl chloride hydrochloride (36.7 mg, 0.22 mmol) and 60% sodium hydride (18 mg, 0.45 mmol) according to standard procedure similar to preparation of compound **14a**. m.p. 223.0–224.8 ℃. ^{1}H NMR (400 MHz, DMSO-d_6): δ 7.53 (s, 1H, H-5'), 7.35 (s, 1H, H-3'), 4.26 (t, J = 5.6 Hz, 2H, OCH_2CH$_2$), 2.98 (q, J = 9.6 Hz, 1H, H-3), 2.83 (s, 2H, OCH$_2$CH_2N), 2.72 (p, J = 7.2 Hz, 1H, H-4β), 2.55 (s, 4H, 2×pyrrolidine-N-CH_2), 2.24 (s, 3H, Ar-CH_3), 2.19 (t, J = 7.2 Hz, 1H, H-7β), 2.11–2.05 (m, 1H, H-2), 1.91 (q, J = 5.6 Hz, 1H, H-5), 1.68–1.58 (m, 7H, 2×pyrrolidine-NCH$_2$CH_2, H-1, 7α, 4α), 1.20 (s, 3H, CH_3-9), 0.92 (s, 3H, CH_3-8), 0.82 (d, J = 6.4 Hz, 3H, CH_3-10)； ^{13}C NMR (100 MHz, CDCl$_3$): δ 151.7 (C=N), 136.1 (C-4'), 133.6 (C-2'), 131.1 (C-5'), 125.3 (C-3'), 73.2 (O*C*H$_2$), 54.6 (OCH$_2$*C*H$_2$N), 54.5 (pyrrolidine-C-2'', 5''), 47.8 (C-3), 41.3 (C-1), 40.4 (C-5), 33.1 (C-6), 32.9 (C-2), 29.6 (C-7), 27.0 (C-4), 23.6 (pyrrolidine-C-3'', 4''), 23.4 (C-9), 20.3 (C-8), 19.8 (C-10), 15.4 (Ar-C). HRMS calcd for $C_{22}H_{35}N_2OS^+$ (M+H$^+$): 375.2465, found: 375.2470. Anal. Calcd. (%)

for $C_{22}H_{35}ClN_2OS$: C, 64.29; H, 8.58; N, 6.82; Found: C, 68.32; H, 8.63; N, 6.78.

4.2 Cytopathic Effect (CPE) Assay Protocol

In CPE assay, MDCK cells were grown to a confluent monolayer in a 96-well culture plate at a concentration of 5×10^4/well for 24 h. The medium was removed, and the cells were rinsed twice. An infectious virus at 100 $TCID_{50}$ was inoculated into the MDCK cells, which were then incubated for 2 h at 37 °C in 5% CO_2. The virus supernatant was then removed, followed by the addition of serial two-fold dilutions of antiviral compounds in DMEM containing 1.5 μg/mL trypsin. After being incubated at 34 °C in 5% CO_2 for 48 h, the infected cells displayed 100% CPE under the microscope, and the CPE percentages in the antiviral compound-treated groups were recorded. The EC_{50} values were calculated using a non-linear regression model in GraphPad Prism 6. All data were obtained for at least three independent experiments.

4.3 Cytotoxicity Assay

Cytotoxicity of compounds was assessed by 3-(4,5-dimethylthiazol-2-yl)-2,5-diphenyltetrazolium bromide (MTT) assay. Madin Darby canine kidney (MDCK) cells on 96-well plates were washed with sterile phosphate buffered saline (PBS). Then 100 μl of the compound in serum-free MEM at two-fold dilution was added to the cells and the cells were incubated in CO_2 incubation at 37 °C. Cell controls were also performed. After 48h, 5 mg/mL of fresh MTT was added to each well and the plates were incubated at 37 ^oC for 4 h. Afterwards, the medium was removed and formazan crystal was dissolved in DMSO (100μl per well). Absorbance of each well at 490 nm was read by a CLARIOstar multi-mode microplate reader (BMG Labtech, Germany). The cell viability (%) = OD of compound well / average OD of control wells. The TC_{50} of each compound was obtained using a non-linear regression model in GraphPad Prism 6.

4.4 Patch clamp assay

The stable cell lines of transformed 293T-Rex expressed WT and S31N mutant M2 channels of avian H5N1 were created by pCDNA4/TO plasmid prior to electrophysiological assay according to the literature. M2-293T-Rex cells was induced with 1 μg/mL tetracycline for 24-48 hours. Patch clamp recordings are performed in

the whole-cell patch clamp configuration at room temperature (23-25 ℃) using an Axopatch 200B amplifier (Molecular Devices) and Digidata 1440A analog-to-digital converter (Molecular Devices). Recording electrodes were pulled from 1.5 mM borosilicate pipettes (World Precision Instruments, Inc., Sarasota, FL) using a horizontal puller (model P-87; Sutter Instrument Company, Novato, CA). The extracellular solution consists of 150 mM NaCl, 1 mM $MgCl_2$, 1 mM $CaCl_2$, 10 mM glucose and 10 mM HEPES. In most of the experiments, the solution was adjusted to pH 6.8 or 10 mM MES was adjusted to pH 5.5 or alternative pH values by the addition of NaOH or HCl. The patch electrode had a resistance of 1.8-2.5 MΩ. The pipet tip was initially filled with amphotericin-free pipet solution containing 130 mM Cs methanesulfonate, 24 mM CsCl, 1 mM $CaCl_2$, 1 mM $MgCl_2$, 10 mM HEPES, and 200 μg/mL amphotericin B. The pH of the intracellular solution was adjusted to 6.8 with CsOH. Clampex 10 (pCLAMP 10, Molecular Devices) was used to control voltage protocols and for data acquisition. Cell concentration was adjusted to 3.3×10^5 cells/ml in PBS (pH 7.4) containing 0.1% BSA, and 30 μl of cells (1×104) were plated per well. 30 μl solution of chemicals in PBS (pH 7.4) was added into each well and mixed gently. Baseline recording was obtained at pH 7.4 after 10 min incubation. Currents were recorded in final pH 5.5 after the addition of MES buffer (60 μl) at every 45 s at -40 mV. The potency of the chemicals was recorded as percentage inhibition of currents observed 2 min after applying 100 μM compounds and the measurements were repeated three times.

4.5 Docking Simulation

The docking calculations were set up with the Schrödinger 2017-1 suite. The recommended procedures from Schrödinger for IFD were followed. The ligand structures were built using the Maestro visualization software and ionization and tautomeric states at pH 7 were prepared with the LigPrep module, optimizing conformations by MMFF force field. Docking simulation on M2-S31N (PDB ID code: 2LY0) or M2-WT (PDB ID code: 2KQT)) was performed to compare the binding sites of our target compounds with the binding sites of the reference ligand, which was retrieved from PDB bank http://www.rscb.org/pdb. The Protein Preparation Wizard (PrepWizard) in Maestro was employed for preparing the protein structures according

to the recommended protein preparation procedure. All waters and ligands were removed from all protein structures. Energy minimization and refinement of the structure was done up to 0.3 Å RMSD by applying OPLS-2005 force field. Docking studies inducing conformational changes in active sites of proteins were performed with the Induced Fit Docking protocol. Initial docking was performed using Glide SP, ligand van der Waals radii of both receptor and ligand were scaled to 0.5. The maximum of 20 poses per ligand were generated. Protein conformations were then generated with Prime, considering flexible all residues within 5 Å from ligand poses, and the conformations whose energy was up to 30 kcal/mol from the best structure and classified within the first 20 poses were selected for redocking. The final IFD redocking round was then performed with Glide XP. Each complex was then ranked according to the IFD score which considers both the docking energy and solvation energy (IFD Score = Glide Score + 5% PrimeEnergy). Finally, only the most favorable docking pose for each ligand was selected for structural analysis. Figures were prepared with UCSF Chimera interface.

Acknowledgment

This work was supported by The Key Scientific Research Project of Colleges and Universities in Henan Province (NO. 18B350005) and the Key Science and Technology Program of Henan Province, China (NO.182102310258).

References

[1] P. Palese, Influenza: old and new threats, Nat. Med. 10 (2004) S82–S87.

[2] R.A. Medina, A. García-Sastre, Influenza A viruses: new research developments, Nat. Rev. Microbiol. 9 (2011) 590-603.

[3] S. Yamayoshi, Y. Kawaoka, Current and future influenza vaccines, Nat. Med. 25

(2019) 212-220..

[4] C.J. Wei, M.C. Crank, J. Shiver, B.S. Graham, J.R. Mascola, G.J. Nabel, Next-generation influenza vaccines: opportunities and challenges, Nat. Rev. Drug Discovery 19 (2020) 239-252.

[5] E. Krol, M. Rychowska, B. Szewczyk, Antivirals - current trends in fighting influenza, Acta Biochim. Pol. 61 (2014) 495-504.

[6] What you should know about flu antiviral drugs, Centers for Disease Control and Prevention, 2019.https://www.cdc.gov/flu/treatment/whatyoushould.htm. (Accessed 22 April 2019).

[7] T. Lampejo, Influenza and antiviral resistance: an overview, Eur. J. Clin. Microbiol. Infect. Dis. 39 (2020) 1201-1208.

[8] M. Imai, M. Yamashita, Y. Sakai-Tagawa, K. Iwatsuki-Horimoto, M. Kiso, J. Murakami, A. Yasuhara, K. Takada, M. Ito, N. Nakajima, K. Takahashi, T.J.S. Lopes, J. Dutta, Z. Khan, D. Kriti, H. van Bakel, A. Tokita, H. Hagiwara, N. Izumida, H. Kuroki, T. Nishino, N. Wada, M. Koga, E. Adachi, D. Jubishi, H. Hasegawa, Y. Kawaoka, Influenza A variants with reduced susceptibility to baloxavir isolated from Japanese patients are fit and transmit through respiratory droplets, Nat. Microbiol. 5(2020) 27-33.

[9] J. Wang, F. Li, C. Ma, Recent progress in designing inhibitors that target the drug-resistant M2 proton channels from the influenza A viruses, Pept. Sci. 104 (2015) 291-309.

[10] R.-X. Gu, L.A. Liu, D.-Q. Wei, Structural and energetic analysis of drug inhibition of the influenza A M2 proton channel, Trends Pharmacol. Sci. 34 (2013) 571-580.

[11] J.L. Thomaston, W.F. DeGrado, Crystal structure of the drug-resistant S31N influenza M2 proton channel, Pept. Sci. 25 (2016) 1551-4.

[12] J.L. Thomaston, A. Konstantinidi, L.J. Liu, G. Lambrinidis, J.Q. Tan, M. Caffrey, J. Wang, W.F. Degrado, A. Kolocouris, X-ray Crystal structures of the influenza M2 proton channel drug-resistant V27A mutant bound to a spiro-adamantyl amine inhibitor reveal the mechanism of adamantane resistance, Biochemistry 59(4) (2020) 627-634.

[13] P.H. Jalily, M.C. Duncan, D. Fedida, J. Wang, I. Tietjen, Put a cork in it: Plugging the M2 viral ion channel to sink influenza, Antivir. Res. 178 (2020) 104780.

[14] J. Wang, C. Ma, J. Wang, H. Jo, B. Canturk, G. Fiorin, L.H. Pinto, R.A. Lamb, M.L. Klein, W.F. DeGrado, Discovery of novel dual inhibitors of the wild-type and the most prevalent drug-resistant mutant, S31N, of the M2 proton channel from influenza A virus, J. Med. Chem. 56 (2013) 2804-2812.

[15] J. Wang, Y. Wu, C. Ma, G. Fiorin, J. Wang, L.H. Pinto, R.A. Lamb, M.L. Klein, W.F. DeGrado, Structure and inhibition of the drug-resistant S31N mutant of the M2 ion channel of influenza A virus, Proc. Natl Acad. Sci. 110(4) (2013) 1315-1320.

[16] Y. Wu, B. Canturk, H. Jo, C. Ma, E. Gianti, M.L. Klein, L.H. Pinto, R.A. Lamb, G. Fiorin, J. Wang, W.F. DeGrado, Flipping in the pore: Discovery of dual Inhibitors that bind in different orientations to the wild-type versus the S31N mutant of the influenza A virus M2 proton channel, J. Am. Chem. Soc. 136 (2014) 17987-17995.

[17] F. Li, C. Ma, W.F. DeGrado, J. Wang, Discovery of highly potent inhibitors targeting the predominant drug-resistant S31N mutant of the influenza A virus M2 proton channel, J. Med. Chem. 59(3) (2016) 1207-1216.

[18] C. Ma, J. Zhang, J. Wang, Pharmacological characterization of the spectrum of antiviral activity and genetic barrier to drug resistance of M2-S31N channel blockers, Mol. Pharmacol. 90(3) (2016) 188-198.

[19] F. Li, Y. Hu, Y. Wang, C. Ma, J. Wang, Expeditious lead optimization of isoxazole-containing influenza A virus M2-S31N inhibitors using the Suzuki–Miyaura cross-coupling reaction, J. Med. Chem. 60(2017) 1580-1590.

[20] Y. Hu, R.K. Hau, Y. Wang, P. Tuohy, Y. Zhang, S. Xu, C. Ma, J. Wang, Structure–property relationship studies of influenza A virus AM2-S31N proton channel blockers, ACS Med. Chem. Lett. 9(11) (2018) 1111-1116.

[21] Y. Wang, Y. Hu, S. Xu, Y. Zhang, R. Musharrafieh, R.K. Hau, C. Ma, J. Wang, In vitro pharmacokinetic optimizations of AM2-S31N channel blockers led to the discovery of slow-binding inhibitors with potent antiviral activity against drug-

resistant influenza A viruses, J. Med. Chem. 61(2018) 1074-1085.

[22] R. Musharrafieh, C. Ma, J. Wang, Profiling the in vitro drug-resistance mechanism of influenza A viruses towards the AM2-S31N proton channel blockers, Antivir. Res. 153 (2018) 10-22.

[23] W. Hu, S. Zeng, C. Li, Y. Jie, Z. Li, L. Chen, Identification of hits as matrix-2 protein inhibitors through the focused screening of a small primary amine library, J. Med. Chem. 53(9) (2010) 3831-3834.

[24] X. Zhao, C. Li, S. Zeng, W. Hu, Discovery of highly potent agents against influenza A virus, Eur. J. Med. Chem. 46(1) (2011) 52-57.

[25] X. Zhao, Y. Jie, M.R. Rosenberg, J. Wan, S. Zeng, W. Cui, Y. Xiao, Z. Li, Z. Tu, M.G. Casarotto, W. Hu, Design and synthesis of pinanamine derivatives as anti-influenza A M2 ion channel inhibitors, Antivir. Res. 96(2) (2012) 91-99.

[26] J. Dong, S. Chen, R. Li, W. Cui, H. Jiang, Y. Ling, Z. Yang, W. Hu, Imidazole-based pinanamine derivatives: Discovery of dual inhibitors of the wild-type and drug-resistant mutant of the influenza A virus, Eur. J. Med. Chem. 108 (2016) 605-615.

[27] X. Zhao, R. Li, Y. Zhou, M. Xiao, C. Ma, Z. Yang, S. Zeng, Q. Du, C. Yang, H. Jiang, Y. Hu, K. Wang, C.K.P. Mok, P. Sun, J. Dong, W. Cui, J. Wang, Y. Tu, Z. Yang, W. Hu, Discovery of highly potent pinanamine-based inhibitors against amantadine- and oseltamivir-resistant influenza A viruses, J. Med. Chem. 61(12) (2018) 5187-5198.

[28] A. Kolocouris, C. Tzitzoglaki, F.B. Johnson, R. Zell, A.K. Wright, T.A. Cross, I. Tietjen, D. Fedida, D.D. Busath, Aminoadamantanes with persistent in vitro efficacy against H1N1 (2009) influenza A, J. Med. Chem. 57(11) (2014) 4629-4639.

[29] E. Torres, R. Leiva, S. Gazzarrini, M. Rey-Carrizo, M. Frigolé-Vivas, A. Moroni, L. Naesens, S. Vázquez, Azapropellanes with anti-influenza A virus activity, ACS Med. Chem. Lett. 5(7) (2014) 831-836.

[30] X. Zhao, Z.-W. Zhang, W. Cui, S. Chen, Y. Zhou, J. Dong, Y. Jie, J. Wan, Y. Xu, W. Hu, Identification of camphor derivatives as novel M2 ion channel inhibitors of influenza A virus, Med.Chem.Comm. 6(4) (2015) 727-731.

[31] W.L. Whipple, H.J. Reich, Use of *N,N′*-dimethoxy-*N,N′*-dimethylurea as a carbonyl dication equivalent in organometallic addition reactions. Synthesis of unsymmetrical ketones, J. Org. Chem. 56(8) (1991) 2911-2912.

[32] M. Wierzbicki, F. Sauveur, J. Bonnet, M. Brisset, C. Tordjman, Thiophene compounds, compositions and use, 1991. US5061704.

[33] B.A. Trofimov, E.Y. Schmidt, N.V. Zorina, E.Y. Senotrusova, N.I. Protsuk, I.A. Ushakov, A.b.I. Mikhaleva, R. Méallet-Renault, G. Clavier, A short-cut from 1-acetyl adamantane to 2-(1-adamantyl)pyrroles, Tetrahedron Lett. 49(28) (2008) 4362-4365.

[34] D.R. Smith, M. Maienthal, J. Tipton, Reduction of oximes with lithium aluminum hydride, J. Org. Chem. 17(2) (1952) 294-297.

[35] A.S. Demir, Ö. Sesenoglu, D. Ülkü, C. Arici, Enantioselective synthesis of 2-(2-arylcyclopropyl)glycines: Conformationally restricted homophenylalanine analogs, Helv. Chim. Acta 87(1) (2004) 106-119.

[36] N.K. Shinada, A.G. de Brevern, P. Schmidtke, Halogens in protein–ligand binding mechanism: A structural perspective, J. Med. Chem. 62(21) (2019) 9341-9356.

[37] J. Wang, C. Ma, V. Balannik, L.H. Pinto, R.A. Lamb, W.F. DeGrado, Exploring the requirements for the hydrophobic scaffold and polar amine in inhibitors of M2 from influenza A virus, ACS Med. Chem. Lett. 2(4) (2011) 307-312.

[38] C.F. Li, Y. Long, Z.X. Lin, Y.L. Jie, Y.J. Xiao, L.Z. Yang, J.J. Sun, Y.Z. Ren, L. Chen, Z.Y. Li, New strategy for high throughput screening of anti-influenza virus M2 ion channel inhibitors, Curr. Pharm. Des. 19(28) (2013) 5146-5155.

[39] W. Sherman, T. Day, M.P. Jacobson, R.A. Friesner, R. Farid, Novel procedure for modeling ligand/receptor induced fit effects, J. Med. Chem. 49(2) (2006) 534-553.

[40] E.F. Pettersen, T.D. Goddard, C.C. Huang, G.S. Couch, D.M. Greenblatt, E.C. Meng, T.E. Ferrin, UCSF Chimera—A visualization system for exploratory research and analysis, J. Comput. Chem. 25(13) (2004) 1605-1612.

[41] Q. Zhang, Z. Xu, W. Zhu, The underestimated halogen bonds forming with protein side chains in drug discovery and design, J. Chem. Inf. Model.57(1) (2017) 22-26.

[42] S.D. Cady, K. Schmidt-Rohr, J. Wang, C.S. Soto, W.F. DeGrado, M. Hong,

Structure of the amantadine binding site of influenza M2 proton channels in lipid bilayers, Nature 463(7281) (2010) 689-692.

Graphical abstract

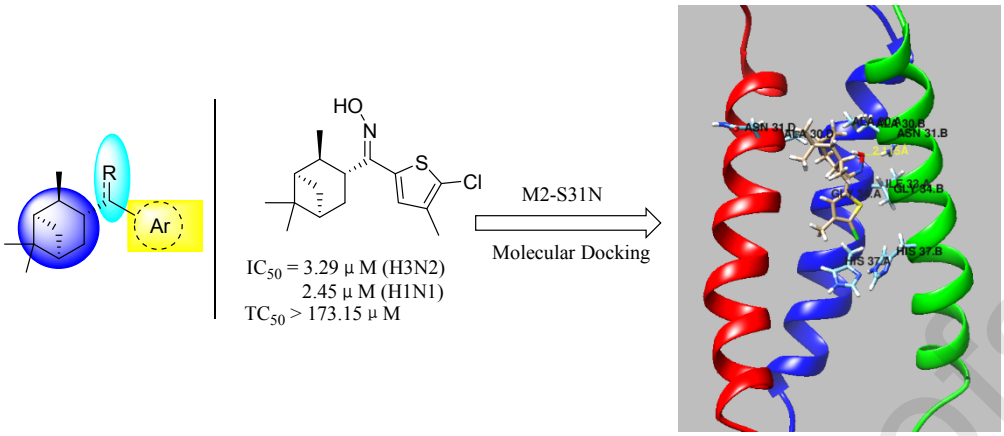

IC_{50} = 3.29 μ M (H3N2)
2.45 μ M (H1N1)
TC_{50} > 173.15 μ M

Research Highlights

A series of pinane oxime derivatives were tested for anti-influenza virus activity and their cytotoxicity in vitro.

Compound **11h** possessed excellent activity with IC_{50} value at the low-micromolar level against both H3N2 and H1N1, with low cytotoxicity

Compound **11h** was identified to be a M2-S31N inhibitor.

The plausible binding mode of compound **11h** was also discussed**.**